Bulletin of the Earthquake
Research Institute
University of Tokyo
Vol. 61 (1986) pp. 429-473

Multiple Tension-Crack Model for Dilatancy: Surface Displacement, Gravity and Magnetic Change

Yoichi Sasai
Earthquake Research Institute
(Received July 28, 1986)

Abstract

A macroscopic model for crustal dilatancy is presented: i.e. Gaussian distribution of small tension-cracks. The influence of a single crack is evaluated by an appropriate strain nucleus in a semi-infinite elastic medium. The effect of all the cracks is given simply by integrating it with the weight of Gaussian distribution. This is nothing but an extension of the multiple Mogi model proposed by Hagiwara (1977b). Three kinds of cracks are adopted: (a) the spherical (i.e. the Mogi model), (b) the T33-type (horizontal penny-shaped cracks) and (c) the T11-type (vertical penny-shaped cracks). The multiple Mogi model composed of spherical cracks is mechanically equivalent to the case where tensile cracks are oriented in every direction. Mechanical distortion of the elastomagnetic half-space gives rise to changes in the gravity and magnetic fields. All these distortion-related quantities are formulated in a unified way. The multiple Mogi and T33-crack models result in changes similar to each other. The only exception is the magnetic total field change: the multiple Mogi model is dominated by overall decrease, while the multiple T33-crack one exhibits practically no field change. On the other hand, the multiple T11-crack model differs substantially from the foregoing two. The upheaval has two humps in some cases and there appears a positive region in the magnetic change. In particular, the gravity field varies remarkably as compared with the height change. The multiple tension-crack model is applicable to volcanic phenomena. It also works as a source model for swarm earthquakes in volcanic regions and certain kinds of magma reservoirs.

1. Introduction

The dilatancy model of earthquake precursors was originally proposed by Nur (1972) and Aggarwal *et al.* (1973) to interpret seismic velocity changes prior to earthquakes. Besides the velocity change, various precursory phenomena looked upon to be explained by more sophisticated

versions of the model: i.e. the dilatancy-diffusion (SCHOLZ *et al.* 1973, ANDERSON and WHITCOMB 1973) and the diffusionless (dry) dilatancy model (STUART 1974, MJACHKIN *et al.* 1975).

Precise measurement of the P wave velocity with explosion techniques did not always support premonitory changes (e.g. the 1978 Izu-Oshima Earthquake of M 7.0: GEOLOGICAL SURVEY OF JAPAN 1979). MOGI (1985) cast doubts on the reliability of some "precursor" events such as the crustal uplift preceding the Niigata earthquake and the electrical resistivity changes in the Garm region, on the basis of which the dilatancy (−diffusion) model was set up.

All these negative examples imply, however, the crack growth does not take place within a sufficiently large volume, several times as much as the focal region. Since the dilatancy itself is usually observed as a forerunner to the failure of intact rocks (BRACE *et al.* 1966), the possibility still remains that it does occur in a small scale volume near active faults by local stress concentration.

Phenomena associated with the dilatancy in crustal rocks are classified into two categories. One is the change in material properties of the medium such as the seismic velocity, the electrical resistivity and some chemical changes including radon emission. The other is the mechanical distorsion, e.g. uplift, horizontal displacement and strain changes. The gravity and magnetic changes are also anticipated in association with resulting mass movement and stresses. Although the magnetic field may possibly be generated by the electrokinetic effect along with the water percolation (MIZUTANI and ISHIDO 1976), we will take into account here only the piezomagnetic effect of strained rocks (STACEY 1964, NAGATA 1970).

Distortion-related phenomena can be dealt with in a unified way. We may simulate the crustal dilatancy by distributing small tensile cracks within a semi-infinite elastic medium. The effect of cracks is approximated by replacing appropriate strain nuclei. We may evaluate the resultant effect of all the cracks simply by integrating the influence function of a single nucleus with the weight of crack distribution. Such superposition is permissible if cracks are distributed sparsely enough to disregard the mutual coupling.

This kind of modelling has been conducted in an attempt to interpret anomalous crustal uplift in terms of dilatancy. Types of strain nuclei (a) and crack distribution functions (b) differ among several authors. SINGH and SABINA (1975) studied such models as (a) the center of dilatation with (b) uniform spherical and cylindrical distribution. HAGIWARA (1977b) investigated the uplift and related gravity change of the multiple Mogi model, i.e. (a) a cluster of small hydrostatically-pumped spheres

with (b) the Gaussian distribution. Such a source is identical to the center of dilatation (YAMAKAWA 1955, MOGI 1958). YAMAZAKI (1978) adopted (a) the center of dilatation plus double force without moment in the vertical direction within (b) an elliptic disk and an ellipsoid. Yamazaki's strain nucleus corresponds to a vertical opening of horizontally embedded cracks.

HAGIWARA's (1977b) model is versatile enough for various spatial configurations of the dilatant volume which may possibly take place in the actual earth. Moreover, his method of calculating gravity changes is also applicable to the piezomagnetic field (SASAI 1984). The gravity and magnetic observations should provide us with powerful constraints to the model. In fact Hagiwara successfully interpreted the gravity change associated with the Matsushiro uplift in terms of water-saturated pores. The displacement field of the multiple Mogi model was approximately solved by Hagiwara. Its rigorous solution was presented by SASAI (1984), which will be followed in the present study.

We have some comments on the gravity and magnetic change associated with dilatancy. Dilatancy-related gravity changes were qualitatively discussed by NUR (1974) and KISSLINGER (1975) with special reference to the Matsushiro uplift. HAGIWARA (1977a) examined the gravity change due to the Mogi model. The density change was properly taken into account in his study. HAGIWARA's (1977b) solution for the gravity change of the multiple Mogi model is thus a rigorous one, which gives a different result from preceding speculations (i.e. NUR 1974, KISSLINGER 1975). We follow HAGIWARA (1977a, b) in the gravity calculation.

Remanent magnetization changes of rocks due to dilatancy were experimentally investigated by MARTIN *et al.* (1978). Their results are not directly applicable to the present calculation, because the constitutive relationship between the remanence change and all the stress components is not sufficiently established owing to experimental difficulties. One of their results is, however, noticeable: the magnetization varies during the dilatancy creep test with increasing dilatancy under a fixed load. The situation can be modelled as the piezomagnetic change of the medium caused by stresses of new cracks.

YAMAZAKI (1978) emphasized the importance of the dominant orientation of tensile cracks under the triaxial tectonic stress. We will investigate two particular cases: indivisual cracks open vertically or horizontally. Corresponding strain nuclei are given by MARUYAMA (1964). It is also shown, however, that the multiple Mogi model is identical to the case where the crack orientation is uniformly distributed in all directions. Hence we will investigate the surface displacement, gravity and magnetic changes associated with the Gaussian distribution of three typical tensile

cracks, i.e. spherical as well as vertical and horizontal penny-shaped cracks. All these distortion-related quantities are not expressible with elementary functions. They are reduced to one dimensional integrals, which will be numerically evaluated with sufficient accuracy by the double exponential formula (TAKAHASHI and MORI 1974).

The present model is a natural expansion of the multiple Mogi model of HAGIWARA (1977b). We may call it the multiple tension-crack model. In the last section we will briefly discuss its application to volcanic phenomena.

2. Gaussian distribution of tensile cracks

Let us take the Cartesian coordinates (x, y, z), in which the z axis is taken positive downward. A homogeneous and isotropic elastic medium occupies $z>0$. It is also assumed that the uppermost portion of the medium from $z=0$ to $z=H$ (the Curie depth) is uniformly magnetized. Suppose that a small dislocation surface $\Sigma(P)$ exists at a point P within the elastic half-space. The m-th component of the displacement at an arbitrary point Q caused by the dislocation is given by the following Volterra's formula (MARUYAMA 1964):

$$u_m(Q)=\iint_{\Sigma} \Delta u_k(P)\, W^m_{kl}(P, Q)\nu_l(P)d\Sigma \qquad (k, l=1, 2, 3) \tag{2.1}$$

$\Delta u_k(P)$ specifies the displacement discontinuity and ν is a unit normal to Σ. $W^m_{kl}(P, Q)$ is the displacement field produced by the elementary dislocation of the type (kl), which is given explicitly by MARUYAMA (1964). The summation convention applies in this paper.

In the case of tensile cracks, the dislocation vector $\boldsymbol{\Delta u}$ is normal to the surface Σ:

$$\frac{\boldsymbol{\Delta u}}{\Delta u}=\boldsymbol{\nu} \qquad \text{or} \qquad \Delta u_k=\Delta u \nu_k \tag{2.2}$$

Then the sum of products $\Delta u_k W^m_{kl}\nu_l$ becomes

$$\Delta u_k W^m_{kl}\nu_l=\Delta u W^m \tag{2.3}$$

where

$$W^m=W^m_{kl}\nu_k\nu_l \tag{2.4}$$

We assume the crack is small enough to ignore details of crack opening along the dislocation surface. Eq. (2.1) is reduced to

$$\left.\begin{aligned} u_m(Q) &= \Delta U W^m(P, Q) \\ \Delta U &= \iint_\Sigma \Delta u(P) d\Sigma \end{aligned}\right\} \tag{2.5}$$

ΔU has a dimension of volume, i.e. the product of average opening distance and crack area. If the crack is penny-shaped with its radius a, $\Delta U = \pi a^2 \Delta u$.

For an arbitrary oriented crack, we need a linear combination of six sets of strain nuclei. We will consider here three particular cases as shown in Fig. 1.

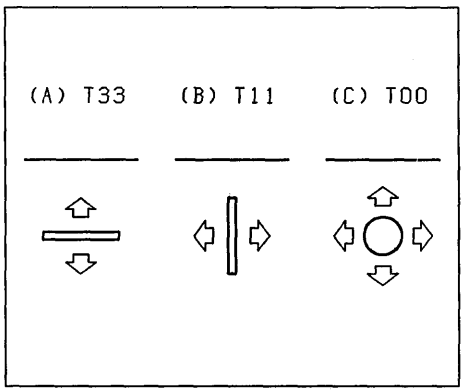

Fig. 1. Three types of tensile cracks: (a) T33 type, (b) T11 type and (c) T00 type.

(a) Horizontal crack (T33 type)

Suppose that a penny-shaped crack is embedded horizontally and it opens in the vertical direction. Since $\nu=(0, 0, 1)$, W^m is reduced to only one term, i.e. $W^m = W^m_{33}$. We call this sort of crack the T33 type crack.

(b) Vertical crack (T11 type)

A crack is placed within a vertical plane and it opens in the horizontal direction. Since $\nu=(\nu_1, \nu_2, 0)$, $W^m = W^m_{11}\nu_1^2 + 2W^m_{12}\nu_1\nu_2 + W^m_{22}\nu_2^2$. Without loss of generality, however, we may put $\nu=(1, 0, 0)$ by rotating the coordinates. The W^m is given simply by W^m_{11}. The crack lies within the $y-z$ plane and it opens in the x direction. We call it the T11 type crack.

(c) Spherical crack (the Mogi model or T00 type)

Instead of the dislocation Σ, we may assume a small sphere at P, pressurized hydrostatically from the inside. This can be a simple mechanical model of the magma reservoir (MOGI 1958). Its displacement field, say W^m_{00}, is equivalent to that produced by the center of dilatation at P

(YAMAKAWA 1955). The sum of three perpendicular A nuclei (i.e. $k=l$ type) is reduced to the center of dilatation, and hence $W_{00}^{m} \propto W_{11}^{m}+W_{22}^{m}+W_{33}^{m}$ (MARUYAMA 1964). We are to investigate the displacement field caused by the Gaussian distribution of microcracks. If each crack is oriented in an arbitrary but uniformly distributed direction, its displacement field is equivalent to that of a strain nucleus which may be derived by averaging direction cosines in equation (2.4) over the entire unit hemispherical surface. Since

$$\iint_{|\Omega|/2} \nu_k \nu_l d\Omega = \begin{cases} \frac{2}{3}\pi & (k=l) \\ 0 & (k \neq l) \end{cases} \tag{2.6}$$

we have

$$W_{00}^{m} \propto \iint_{|\Omega|/2} W_{kl} \nu_k \nu_l d\Omega \tag{2.7}$$

The displacement field by a cluster of small expanding spheres is quite equivalent to that by tensile cracks with a uniformly scattered orientation.

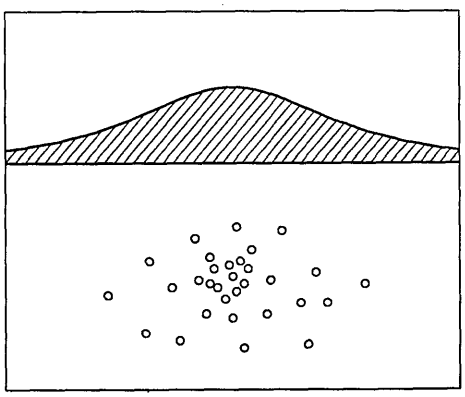

Fig. 2. A schematic view of the multiple tension-crack model.

Suppose a number of microcracks are distributed in Gaussian centered at $(0, 0, D)$. See Fig. 2. We assume the variance σ_r^2 in the horizontal distribution is isotropic and the vertical variance σ_z^2 differs from σ_r^2. The distribution function is given by

$$\left.\begin{aligned} p(x, y) &= \frac{1}{2\pi \sigma_r^2} \exp\left(-\frac{x^2+y^2}{2\sigma_r^2}\right) \\ q(z) &= \frac{1}{\sqrt{2\pi}\,\sigma_z} \exp\left\{-\frac{(D-z)^2}{\sqrt{2}\,\sigma_z^2}\right\} \end{aligned}\right\} \tag{2.8}$$

Quantities related to the mechanical distortion are given by the displacement field itself due to appropriate strain nuclei and/or its derivatives. Let us put such an influence function $f(x, y, z, z')$, which represents the effect of a single crack placed at $(0, 0, z')$. The effect of total cracks under the distribution (2.8) is given by

$$g(x, y, z)=\int_0^\infty q(z')F(x, y, z, z')dz' \tag{2.9}$$

where

$$F(x, y, z, z')=\iint_{-\infty}^{\infty} f(x-x', y-y', z-z')p(x', y')dx'dy' \tag{2.10}$$

The convolution integral (2.10) can be evaluated by the Fourier transform method.

Surface uplift and horizontal displacement can be obtained by substituting the displacement field of a particular strain nucleus into f in eq. (2.10). Strains such as tilt, extension and volumetric strain are easily derived by differentiation. We will not deal with strain changes in this paper.

Let us describe how to estimate the gravity and magnetic field changes. HAGIWARA (1977a) obtained the gravity change associated with the Mogi model. The solution consists of four terms: i.e. the free-air change proportional to the uplift (G1), the Bouguer change caused by the upheaved portion of the ground (G2), the gravitational attraction of the material filling the expanding part of the source sphere (G3), and the gravity field due to the density changes in the elastic half space (G4). Correspondingly the magnetic change has four terms: free-air magnetic change along with departure of the observation site from the

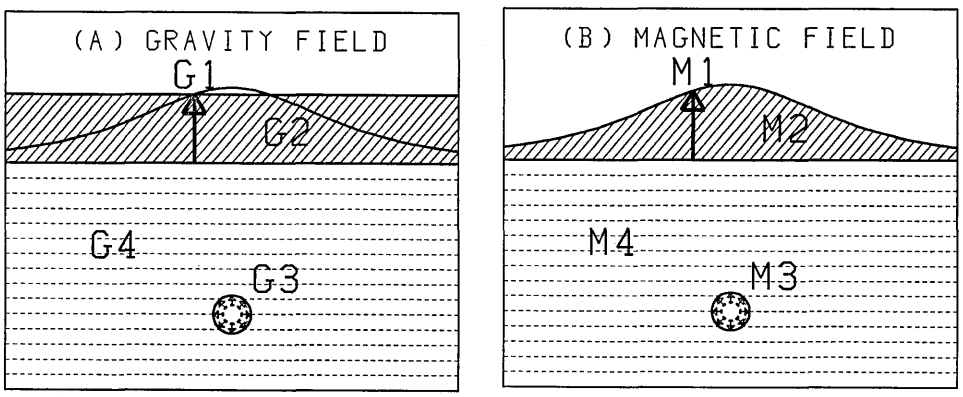

Fig. 3. A schematic representation of the four kinds of contributions to (a) gravity and (b) magnetic change.

geocentric dipole (M1), the magnetic anomaly produced by the surface topography of the upheaval (M2), the effect of a void representing the source volume change (M3), and the piezomagnetic effect caused by the stress-induced magnetization of the top magnetic layer (M4). A schematic illustration is given in Fig. 3(a) for the gravity and 3(b) for the magnetic changes.

HAGIWARA (1977a) demonstrated $|G1|>|G2|>|G3|>|G4|$ when the source sphere was filled with gas, and $|G1|>|G2|>|G4|>|G3|$ when filled with magma. Accordingly the gravity data bears information on the material density filling the crack. In the case of the magnetic change, the crack is regarded simply as a void because gas, water and magma are non-magnetic. SASAI (1985) showed $|M4| \gg |M2| \sim |M3| \gg |M1|$ for the Mogi model. This feature is common even for T11 and T33 cracks.

In general the stress tensor T is subdivided into the sum of the average stress σ_0 and the stress deviation T':

$$T=\sigma_0 E+T' \tag{2.11}$$

where E is a unit matrix and

$$\left.\begin{aligned} \sigma_0&=\frac{1}{3}(\tau_{xx}+\tau_{yy}+\tau_{zz}) \\ T'&=\begin{bmatrix} \tau_{xx}-\sigma_0 & \tau_{xy} & \tau_{xz} \\ \tau_{yx} & \tau_{yy}-\sigma_0 & \tau_{yz} \\ \tau_{zx} & \tau_{zy} & \tau_{zz}-\sigma_0 \end{bmatrix} \end{aligned}\right\} \tag{2.12}$$

σ_0 produces the density change and hence G4. On the other hand, T' is the causative of the piezomagnetic field M4. In fact we have

$$\Delta J=\frac{3}{2}\beta T'J \tag{2.13}$$

in which ΔJ is the stress-induced magnetization produced within the initial magnetization J and β is the stress sensitivity (SASAI 1980, 1983). Thus the information on the stress field involved in gravity and magnetic data is complementary to each other.

G3 and G4 bear valuable information, although their contributions to the total gravity change are less than those of G1 and G2. We will evaluate all the terms of the gravity change for the three types of tensile cracks. According to SASAI (1985), however, M4 is predominant in the magnetic change, while the remainder are negligible. We will calculate only M4 for the magnetic field. Elementary piezomagnetic potentials (SASAI 1980) are used for the present purpose. Owing to the

property (2.13), the magnetic change is highly sensitive to the character of the stress field. We will find later on that it varies quite differently for the different types of cracks.

We have thus extended HAGIWARA's (1977b) model. It is characterized by three parameters $\{\sigma_r, \sigma_z, D\}$ as well as three different kind of cracks. We may simulate various situations of the crustal dilatancy by the present model. The only defect is that the distribution is symmetric in the horizontal direction ($\sigma_x=\sigma_y=\sigma_r$). It could be overcome, however, by arranging some crack assemblages transversly.

3. The multiple Mogi model

Let us investigate the multiple Mogi model, originally proposed by HAGIWARA (1977b). We will first derive an expression for the crustal uplift. When a small sphere at (x', y', z') expands hydrostatically, the uplift Δh_p at a surface point $(x, y, 0)$ is given by (YAMAKAWA 1955)

$$\Delta h_p(x, y)=-\frac{\lambda+2\mu}{2\mu(\lambda+\mu)}a^3\Delta P\frac{z'}{\{(x-x')^2+(y-y')^2+z'^2\}^{3/2}} \tag{3.1}$$

where λ and μ are Lamé's constants, a the radius of a sphere and ΔP the internal pressure of the sphere. Substituting (3.1) into f in eq. (2.11), we obtain the resultant uplift ΔH_{00} (x, y) as follows:

$$\Delta H_{00}(x, y)=-\frac{\lambda+2\mu}{2\mu(\lambda+\mu)}a^3\Delta P\int_0^\infty q(z')F(x, y, z')dz' \tag{3.2}$$

where

$$F(x, y, z')=\iint_{-\infty}^{\infty}\frac{z'}{\{(x-x')^2+(y-y')^2+z'^2\}^{3/2}}p(x', y')dx'dy' \tag{3.3}$$

We now apply the Fourier transform method to evaluate the convolution integral (3.3). We denote the Fourier transform of a function f by placing an asterisk to the right and top of the letter f (e.g. f^*). We follow the definition of the Fourier transform and its inverse as

$$\left.\begin{aligned} f^*(k_1, k_2)&=\frac{1}{2\pi}\iint_{-\infty}^{\infty}f(x, y)e^{-i(k_1x+k_2y)}dxdy \\ f(x, y)&=\frac{1}{2\pi}\iint_{-\infty}^{\infty}f^*(k_1, k_2)e^{i(k_1x+k_2y)}dk_1dk_2 \end{aligned}\right\} \tag{3.4}$$

The Fourier transform of a convolution $f*g$ is given by

$$(f*g)^*=2\pi f^*g^* \tag{3.5}$$

Since

$$p^*(k_1, k_2)=\frac{1}{2\pi}\exp\left(-\frac{1}{2}\sigma_r^2 k^2\right) \tag{3.6}$$

$$\Delta h_p^*(k_1, k_2)=-\frac{\lambda+2\mu}{2\mu(\lambda+\mu)}a^3\Delta P e^{-kz'} \tag{3.7}$$

where

$$k^2=k_1^2+k_2^2\ , \tag{3.8}$$

we obtain

$$\left.\begin{aligned}\Delta H_{00}^*(k_1, k_2)&=-\frac{\lambda+2\mu}{2\mu(\lambda+\mu)}a^3\Delta P\int_0^\infty q(z')e^{-kz'}\exp\left(-\frac{1}{2}\sigma_r^2k^2\right)dz'\\&=-\frac{\lambda+2\mu}{2\mu(\lambda+\mu)}a^3\Delta P\exp\left\{-\frac{1}{2}(\sigma_r^2-\sigma_z^2)k^2\right\}e^{-kD}\Phi\left(\frac{-D+\sigma_z^2k}{\sqrt{2}\,\sigma_z}\right)\end{aligned}\right\} \tag{3.9}$$

Φ is defined as

$$\Phi(x)=\frac{1}{\sqrt{\pi}}\int_x^\infty e^{-t^2}dt=\begin{cases}\dfrac{1}{2}erfc(x) & (x\geqq 0)\\[2ex] \dfrac{1}{2}\{1+erf(|x|)\} & (x<0)\end{cases} \tag{3.10}$$

in which $erf(x)$ and $erfc(x)$ are Gauss' error and complementary error function defined for positive x:

$$\left.\begin{aligned}erf(x)&=\frac{2}{\sqrt{\pi}}\int_0^x e^{-t^2}dt\\ erfc(x)&=1-erf(x)\end{aligned}\right\} \tag{3.11}$$

Inverse Fourier transform of eq. (3.9) gives rise to

$$\Delta H_{00}(r)=\int_0^\infty \Delta H_{00}^*(k)J_0(kr)kdk \tag{3.12}$$

Δh_0, the value of ΔH_{00} at $r=0$, gives the maximum uplift:

$$\Delta h_0=-\frac{\lambda+2\mu}{2\mu(\lambda+\mu)}a^3\Delta P\, h_{00} \tag{3.13}$$

where

$$h_{00}=\int_0^\infty \exp\left\{-\frac{1}{2}(\sigma_r^2-\sigma_z^2)k^2\right\}e^{-kD}\Phi\left(\frac{-D+\sigma_z^2k}{\sqrt{2}\,\sigma_z}\right)kdk \tag{3.14}$$

h_{00} is a constant peculiar to the model specified by parameters $\{\sigma_r, \sigma_z, D\}$. All the distortion-related quantities are proportional to the moment of

source spheres, i.e. $a^3\Delta P$ in eq. (3.13). This parameter is not, however, observable. Instead we may give the maximum uplift Δh_0 as a measure of the moment intensity. Eq. (3.12) is rewritten as:

$$\Delta H_{00}(x, y)=\frac{\Delta h_0}{h_{00}}\int_0^\infty Q_1(k)e^{-kD}J_0(kr)kdk \tag{3.15}$$

where

$$Q_1(k)=\exp\left\{-\frac{1}{2}(\sigma_r^2-\sigma_z^2)k^2\right\}\Phi\left(\frac{-D+\sigma_z^2 k}{\sqrt{2}\,\sigma_z}\right) \tag{3.16}$$

Eq. (3.15) is the rigorous solution of crustal uplift caused by the multiple Mogi model. HAGIWARA (1977b) put the Φ term in eq. (3.9) equal to unity assuming σ_z small. He expanded the exponential term in a Taylor series around $k=0$, integrated it by terms and obtained an approximate solution expressed with elementary functions. Hagiwara's approximation is valid only in the limited case $D\gg\sigma_r\geqq\sigma_z$. The general expression of the solution (3.15) is no longer reducible to elementary functions.

If we integrate eq. (3.15) after putting σ_r and σ_z zero, we obtain the uplift due to the single Mogi model placed at $(0, 0, D)$. A question may arise if the integral (3.15) does not converge in case that $\sigma_r<\sigma_z$: the integrand of eq. (3.15) contains a steeply-increasing function $\exp\{1/2(\sigma_z^2-\sigma_r^2)k^2\}$. Actually $erfc(x)$ is a very rapidly-decreasing function: i.e. $xe^{x^2}erfc(x)$ remains finite as x approaches infinity (GAUTSCHI 1964). The integrand of eq. (3.15) decreases with increasing k so that it converges absolutely.

The error and Bessel functions are originally defined in integral forms. In other words, eq. (3.15) is nothing but a formal reduction to one dimensional integral from the volumetric one in eq. (3.2). We have, however, useful mini-max approximation formulae for error and Bessel functions (e.g. HASTINGS 1955) to compute numerical values with sufficient accuracy and speed. The double exponential formula (DEF: TAKAHASHI and MORI 1974) is applied to numerically integrate eq. (3.15).

The horizontal displacement at the surface can be obtained in a similar way. The surface displacement in the x direction due to the center of dilatation at (x', y', z') was solved by YAMAKAWA (1955) as:

$$\Delta x_p(x, y)=-\frac{\lambda+2\mu}{2\mu(\lambda+\mu)}a^3\Delta P\frac{x-x'}{\{(x-x')^2+(y-y')^2+z'^2\}^{3/2}} \tag{3.17}$$

The resultant horizontal displacement in the x direction is given by

$$\Delta X_{00}(x, y) = -\frac{\lambda+2\mu}{2\mu(\lambda+\mu)} a^3 \Delta P \int_0^\infty q(z') F(x, y, z') dz' \tag{3.18}$$

where

$$F(x, y, z') = \iint_{-\infty}^{\infty} \frac{x-x'}{\{(x-x')^2+(y-y')^2+z'^2\}^{3/2}} p(x', y') dx' dy' \tag{3.19}$$

Since

$$\Delta x_p^* = -\frac{\lambda+2\mu}{2\mu(\lambda+\mu)} a^3 \Delta P \left(-\frac{ik_1}{k}\right) e^{-kz'} \tag{3.20}$$

we have

$$\Delta X_{00}^*(k_1, k_2) = -\frac{\lambda+2\mu}{2\mu(\lambda+\mu)} a^3 \Delta P \left(-\frac{ik_1}{k}\right) \exp\left\{-\frac{1}{2}(\sigma_r^2-\sigma_z^2)k^2\right\} \Phi\left(\frac{-D+\sigma_z^2 k}{\sqrt{2}\,\sigma_z}\right) \tag{3.21}$$

Inversion of eq. (3.21) gives

$$\Delta X_{00}(x, y) = \frac{\Delta h_0}{h_{00}} \int_0^\infty \left(-\frac{ik_1}{k}\right) Q_1(k) e^{-kD} J_0(kr) k dk \tag{3.22}$$

The variable k_1 is still involved in eq. (3.22), which can be eliminated as follows. Going back to the original definition of double Fourier transform, we find a relation:

$$\frac{1}{2\pi} \iint_{-\infty}^{\infty} ik_1 f(k) e^{i(k_1 x + k_2 y)} dk_1 dk_2 = -\frac{x}{r} \int_0^\infty f(k) J_1(kr) k^2 dk \tag{3.23}$$

Thus eq. (3.22) is reduced to

$$\Delta X_{00}(x, y) = \frac{\Delta h_0}{h_{00}} \frac{x}{r} \int_0^\infty Q_1(k) e^{-kD} J_1(kr) k dk \tag{3.24}$$

The horizontal displacement in the y direction is obtained in quite the same manner:

$$\Delta Y_{00}(x, y) = \frac{\Delta h_0}{h_{00}} \frac{y}{r} \int_0^\infty Q_1(k) e^{-kD} J_1(kr) k dk \tag{3.25}$$

Finally the displacement in the radial direction results in

$$\Delta R_{00}(x, y) = \frac{\Delta h_0}{h_{00}} \int_0^\infty Q_1(k) e^{-kD} J_1(kr) k dk \tag{3.26}$$

The derivation process of uplift and horizontal displacement makes a prototype for obtaining any other deformation-related quantities.

Gravity change

We will briefly follow how to obtain the gravity change after HAGIWARA (1977a, b). He derived the gravity change rate (i.e. the ratio between the gravity and height change) due to the single Mogi model as

$$\delta g/\Delta h_p = -\gamma + \frac{2\pi G\rho_0(\lambda+\mu)}{\lambda+2\mu} \tag{3.27}$$

γ is the free-air gravity change rate ($\gamma=0.3086$ mgal/m), G the gravitational constant and ρ_0 the material density filling the source sphere. Δh_p is already given in eq. (3.1). As has been discussed in section 2, the gravity change consists of four terms. We will write down each term explicitly (HAGIWARA 1977a):

$$\text{G1}: \qquad \delta g_1(x, y) = -\gamma \Delta h_p(x, y) \tag{3.28a}$$

$$\text{G2}: \qquad \delta g_2(x, y) = 2\pi G\rho \Delta h_p(x, y) \tag{3.28b}$$

$$\text{G3}: \qquad \delta g_3(x, y) = 2\pi G(\rho_0-\rho)\frac{\lambda+\mu}{\lambda+2\mu}\Delta h_p(x, y) \tag{3.28c}$$

$$\text{G4}: \qquad \delta g_4(x, y) = -2\pi G\rho\frac{\mu}{\lambda+2\mu}\Delta h_p(x, y) \tag{3.28d}$$

in which ρ is the density of the elastic medium.

It is easily understood that G1 and G2 are in proportion to height changes, because G1 is by definition and the Bouguer change G2 is approximated by an infinite plate having a thickness equal to the upheaval. For the Mogi model, the uplift Δh_p happened to be of the same functional form as that of the gravitational attraction of a point mass, and hence δg_3 is also proportional to the height change. This is not valid for other types of cracks.

The density change caused by the Mogi model with its source at $(0, 0, z')$ is given by

$$\left.\begin{aligned} \Delta\rho(x, y, z; z') &= -\rho \operatorname{div} \boldsymbol{u} = \rho\frac{a^3\Delta P}{\lambda+\mu}\left\{\frac{1}{R^3}-\frac{3(z+z')}{R^5}\right\} \\ \text{where} \quad R &= \sqrt{x^2+y^2+(z+z')^2} \end{aligned}\right\} \tag{3.29}$$

It produces the gravity field G4:

$$\delta g_4(x, y) = G\int_0^\infty z''dz''\iint_{-\infty}^{\infty}\frac{\Delta\rho(x'', y'', z''; z')}{\{(x-x'')^2+(y-y'')^2+z''^2\}^{3/2}}dx''dy'' \tag{3.30}$$

The convolution integral (3.30) can be solved by the Fourier transform method, which results in eq. (3.28d). This is again proportional to Δh_p. Since other kinds of tensile cracks have different $\Delta\rho, \delta g_4$ is not always so simply related to the uplift.

In the case of the Mogi model, the gravity change at every point on the surface is proportional to the height change at the observation site. The relationship is exactly the same for the multiple Mogi model, since the resultant gravity change δG_{00} is obtained simply by superposition. Thus we have

$$\delta G_{00}/\Delta H_{00}=-\gamma+\frac{2\pi G\rho_0(\lambda+\mu)}{\lambda+2\pi} \tag{3.31}$$

Magnetic change

The piezomagnetic field associated with the Mogi model was solved by SASAI (1979). The magnetic potential at a point (x, y, z) due to a center of dilatation embedded at $(0, 0, \xi_3)$ is given by

$$\frac{w_{00}^z}{C_{00}^z}=\frac{\mu}{2(\lambda+\mu)}\left(\frac{x}{\rho_1^3}-\frac{x}{\rho_3^3}\right)+9H\frac{xD_3}{\rho_3^5}+\begin{cases}0 & (H<\xi_3)\\ \dfrac{3}{2}\left(\dfrac{x}{\rho_1^3}-\dfrac{x}{\rho_2^3}\right) & (H>\xi_3>0)\end{cases} \tag{3.32a}$$

$$\frac{w_{00}^z}{C_{00}^{z1}}=-\frac{\mu}{2(\lambda+\mu)}\left(\frac{D_1}{\rho_1^3}-\frac{D_3}{\rho_3^3}\right)+3H\left(-\frac{1}{\rho_3^3}+\frac{3D_3^2}{\rho_3^5}\right)+\begin{cases}0 & (H<\xi_3)\\ \dfrac{3}{2}\left(\dfrac{D_1}{\rho_1^3}-\dfrac{D_2}{\rho_2^3}\right) & (H>\xi_3>0)\end{cases} \tag{3.32b}$$

where

$$\left.\begin{aligned}&D_1=\xi_3-z,\ D_2=2H-\xi_3-z,\ D_3=2H+\xi_3-z\\ &\rho_i=\sqrt{x^2+y^2+D_i^2}\\ &C_{00}^m=2\pi\beta J_m C_0\quad (m=x, z),\quad C_0=-\frac{1}{2}a^3\Delta P\end{aligned}\right\} \tag{3.33}$$

J_x and J_z are the horizontal and vertical magnetization of the crust respectively. The stress sensitivity β is defined here on the ordinary stress convention in the elasticity (i.e. compression is negative). The negative sign in the definition of C_0 in eq. (3.33) is justified owing to this stress convention.

Exchanging the parameter ξ_3 for z', we may substitute w^x_{00} and w^z_{00} into f in eq. (2.10). We can evaluate the convolution integrals by the same procedure we used in the surface displacement. Fourier transforms of (3.32a) and (3.32b) are given in Appendix A. Piezomagnetic potentials due to the multiple Mogi model are as follows:

$$W^x_{00}/C^x_{00}=-\frac{x}{r}\int_0^\infty \overline{W}^x_{00}(k,z)J_1(kr)k^2dk \tag{3.34a}$$

$$W^z_{00}/C^z_{00}=\int_0^\infty \overline{W}^z_{00}(k,z)J_0(kr)kdk \tag{3.34b}$$

$\overline{W}^x_{00}(k,z)$ and $\overline{W}^z_{00}(k,z)$ are summarized in Appendix B. With the aid of the relationship (3.13), C^m_{00} in eq. (3.34) is reduced to

$$C^m_{00}=2\pi\frac{\lambda+\mu}{\lambda+2\mu}\mu\beta J_m\frac{\Delta h_0}{h_{00}} \tag{3.34c}$$

The magnetic field is given by differentiation of potentials (3.34). We denote three components of the magnetic field in association with J_x and J_z as (x_H, y_H, z_H) and (x_V, y_V, z_V) respectively. They are represented as

$$x_H=A+\frac{x^2}{r^2}(B-2A),\ y_H=\frac{xy}{r^2}(B-2A),\ z_H=Cx \tag{3.35a}$$

$$x_V=Dx, \qquad y_V=Dy, \qquad z_V=-E \tag{3.35b}$$

where

$$\left.\begin{aligned}
A(r,z)&=\int_0^\infty \overline{W}^z_{00}(k,z)\frac{J_1(kr)}{r}k^2dk\\
B(r,z)&=\int_0^\infty \overline{W}^z_{00}(k,z)J_0(kr)k^3dk\\
C(r,z)&=\int_0^\infty \overline{W}^z_{00}(k,z)\frac{J_1(kr)}{r}k^3dk\\
D(r,z)&=\int_0^\infty \overline{W}^z_{00}(k,z)\frac{J_1(kr)}{r}k^2dk\\
E(r,z)&=\int_0^\infty \overline{W}^z_{00}(k,z)J_0(kr)k^2dk
\end{aligned}\right\} \tag{3.36}$$

Some of eqs. (3.35) and (3.36) look apparently indefinite at $r=0$. Taking into account the characteristics of the Bessel function

$$\lim_{r\to 0}J_1(kr)/r=\frac{1}{2}k,\quad \lim_{r\to 0}J_0(kr)=1 \tag{3.37}$$

we find all of them are convergent at $r=0$. In particular $B=2A$ (at $r=0$), and hence we have

$$x_H(r=0)=A(r=0),\quad y_H(r=0)=0 \tag{3.38}$$

4. The multiple T33 crack model

This type of crack was investigated in detail by YAMAZAKI (1978). It effectively produces the surface uplift. The opening of a crack tends to occur in the direction of the minimum compressive stress. The T33 crack develops under a stress field where compression prevails horizontally. Thrust faulting should take place under such circumstances.

The displacement field due to a single T33 crack is given for the Poisson solid case ($\lambda=\mu$) by MARUYAMA (1964). We may follow MARUYAMA (1964) to get the displacement and its Fourier transform via an appropriate Galerkin vector even for arbitrary λ and μ.

The displacement field $\boldsymbol{u}$ is derived from the corresponding Galerkin vector $\boldsymbol{\Gamma}(\Gamma_1, \Gamma_2, \Gamma_3)$ as:

$$\boldsymbol{u}=(\nabla^2-\alpha\, grad\, div)\boldsymbol{\Gamma} \tag{4.1}$$

where

$$\alpha=\frac{\lambda+\mu}{\lambda+2\mu} \tag{4.2}$$

Fourier transforms of the displacement field can be represented by

$$\left.\begin{aligned} u_x^* &= (\alpha k_1^2-k^2+p^2)\Gamma_1^*+\alpha k_1k_2\Gamma_2^*-\alpha ik_1p\Gamma_3^* \\ u_y^* &= \alpha k_1k_2\Gamma_1^*+(\alpha k_2^2-k^2+p^2)\Gamma_2^*-\alpha ik_2p\Gamma_3^* \\ u_z^* &= -\alpha ik_1p\Gamma_1^*-\alpha ik_2p\Gamma_2^*+(-k^2+(1-\alpha)p^2)\Gamma_3^* \end{aligned}\right\} \tag{4.3}$$

in which p is a differential operator:

$$p\equiv\frac{\partial}{\partial z} \tag{4.4}$$

We will later require $div\, \boldsymbol{u}$ for computing δg_4. Its Pourier transform is given by

$$(div\, \boldsymbol{u})^*=(1-\alpha)(p^2-k^2)(ik_1\Gamma_1^*+ik_2\Gamma_2^*+p\Gamma_3^*) \tag{4.5}$$

The Galerkin vector for the T33 type strain nucleus has already been given by MARUYAMA (1964). We must, however, deal with its Fourier transform in the sense of distribution or generalized functions (see text, for example, VLADIMIROV 1971). Some problems related to its

application are discussed in the derivation process of elementary piezomagnetic potentials (SASAI 1980).

The Fourier transforms (4.3) and (4.5) are summarized in Appendix A. Transforms for the surface uplift and horizontal displacement Δh_p^* and Δx_p^* are also given. In the case of the T33 type crack, the surface displacement is irrespective of whether λ and μ are equal or not.

The surface displacement due to the Gaussian distribution of T33 cracks can be derived in quite the same manner as in section 3. Only the results are presented here:

Uplift

$$\Delta H_{33}=\frac{\Delta h_0}{h_{33}}\int_0^\infty\left\{\frac{\sigma_z}{\sqrt{2\pi}}k\exp\left(-\frac{1}{2}\sigma_r{}^2k^2-\frac{D^2}{2\sigma_z{}^2}\right)\right.$$
$$\left.+(-\sigma_z{}^2k^2+Dk+1)e^{-kD}Q_1(k)\right\}J_0(kr)kdk \tag{4.6}$$

Horizontal displacement in the x direction

$$\Delta X_{33}=\frac{\Delta h_0}{h_{33}}\frac{x}{r}\int_0^\infty\left\{\frac{\sigma_z}{\sqrt{2\pi}}\exp\left(-\frac{1}{2}\sigma_r{}^2k^2-\frac{D^2}{2\sigma_z{}^2}\right)\right.$$
$$\left.+(D-k\sigma_z{}^2)e^{-kD}Q_1(k)\right\}J_1(kr)k^2dk \tag{4.7}$$

Horizontal displacement in the y direction

$$\Delta Y_{33}=\Delta X_{33}(x\leftrightarrow y) \tag{4.8}$$

where

$$h_{33}=\int_0^\infty\left\{\frac{\sigma_z}{\sqrt{2\pi}}k\exp\left(-\frac{1}{2}\sigma_r{}^2k^2-\frac{D^2}{2\sigma_z{}^2}\right)\right.$$
$$\left.+(-\sigma_z{}^2k^2+Dk+1)e^{-kD}Q_1(k)\right\}kdk \tag{4.9}$$

Gravity change

Let us first investigate the gravity change caused by a single T33 crack. By definition, G1 and G2 are proportional to the upheaval at the observation site and are given as follows:

$$\text{G1}: \qquad \delta g_1=-\gamma\Delta h_p(x, y) \tag{4.10}$$

$$\text{G2}: \qquad \delta g_2=2\pi G\rho\Delta h_p(x, y) \tag{4.11}$$

where the uplift due to a T33 crack is given by

$$\Delta h_p(x, y)=\frac{3}{2\pi}\Delta U\frac{\xi_3^3}{R^5} \tag{4.12}$$

The incremental crack volume may be approximated by a circular disk. Although the gravitational attraction of a circular disk is given by SINGH (1977), it can be regarded as the gravity of a point mass of $\Delta U(\rho_0-\rho)$ when the crack is small. In this case G3 is given simply as

$$\text{G3}: \qquad \delta g_3=\Delta U(\rho_0-\rho)G\frac{\xi_3}{R^3} \tag{4.13}$$

Referring to (4.12), we find δg_3 is not proportional to the uplift.

Finally G4, the gravity field due to density changes, is expressed by

$$\delta g_4=-\rho G\int_0^\infty z'dz'\iint_{-\infty}^{\infty}\frac{div\ \boldsymbol{U}_{33}(x', y', z')}{\{(x-x')^2+(y-y')^2+z'^2\}^{3/2}}dx'dy' \tag{4.14}$$

With the aid of $(div\ \boldsymbol{U}_{33})^*$ in Appendix A, we obtain its Fourier transform as

$$\begin{aligned}\delta g_4^* &= \rho G\Delta U\int_0^\infty\left[(1-\alpha)ke^{-k\zeta_1}-\{(1+\alpha)k+2k^2\xi_3\}e^{-k\zeta_2}\right]e^{-kz'}dz' \\ &= -\rho G\Delta U\alpha(1+k\xi_3)e^{-k\xi_3}\end{aligned} \tag{4.15}$$

Inversion of eq. (4.15) gives

$$\text{G4}: \qquad \delta g_4=-3\rho G\Delta U\alpha\frac{\xi_3^3}{R^5}=-2\pi\rho G\alpha\Delta h_p(x, y) \tag{4.16}$$

The G4 term due to a T33 crack is again proportional to the uplift as we have seen in the case of the Mogi model. Its proportional constant differs from that of the Mogi model (cp. eq. (3.28d)).

The total gravity change by a single T33 crack is thus given by

$$\delta g=\left(-\gamma+2\pi G\rho\frac{\mu}{\lambda+2\mu}\right)\Delta h_p+\Delta U(\rho_0-\rho)G\frac{\xi_3}{R^3} \tag{4.17}$$

The gravity change associated with the multiple T33 crack model can be subdivided into a part proportional to the upheaval and a minor non-proportional one. The contribution from the last term on the righthand side of eq. (4.17), δG_3 say, can be estimated in quite the same way as we have obtained the uplift due to the multiple Mogi model, exclusive of its coefficient:

$$\delta G_3=\Delta U(\rho_0-\rho)G\int_0^\infty Q_1(k)e^{-kD}J_0(kr)kdk \tag{4.18}$$

The unknown factor ΔU can be replaced with an observable quantity Δh_0. Hence the total gravity change δG_{33} due to the multiple T33 crack model is reduced to

$$\delta G_{33}=\left(-\gamma+2\pi\rho G\frac{\mu}{\lambda+2\mu}\right)\Delta H_{33}(x, y)$$
$$+2\pi(\rho_0-\rho)G\frac{\Delta h_0}{h_{33}}\int_0^\infty Q_1(k)e^{-kD}J_0(kr)kdk \qquad (4.19)$$

Magnetic change

Elementary piezomagnetic potentials due to a T33 type strain nucleus are obtained from SASAI (1980). They are not reproduced here because of their lengthiness. We need Fourier transforms of potentials, which are found in Appendix A. The same procedure as we have followed in the multiple Mogi model leads to the magnetic potential associated with the multiple T33 crack model as

$$W^x_{33}/C^x_{33}=-\frac{x}{r}\int_0^\infty \overline{W}^z_{33}(k, z)J_1(kr)k^2dk \qquad (4.20a)$$

$$W^z_{33}/C^z_{33}=\int_0^\infty \overline{W}^z_{33}(k, z)J_0(kr)kdk \qquad (4.20b)$$

where

$$C^m_{33}=-\frac{1}{2}\mu\beta J_m\frac{\Delta h_0}{h_{33}} \qquad (m=x, z) \qquad (4.21)$$

$\overline{W}^x_{33}$ and $\overline{W}^z_{33}$ are given in Appendix B. We need a comment on the negative sign on the righthand side of eq. (4.21). In SASAI's (1980) paper, the stress convention for β is opposite in sign to MARUYAMA'S (1964) stress field solution: β is defined positive for compression, while the latter is negative. The negative sign in eq. (4.21) is thus introduced to accomodate the discrepancy.

Magnetic components are derived by differentiating (4.20). They are expressed by eq. (3.35) and (3.36), in which we have to replace $\overline{W}^z_{00}$ and $\overline{W}^z_{00}$ with $\overline{W}^x_{33}$ and $\overline{W}^z_{33}$ respectively.

In fact, the T33 crack produces almost no appreciable magnetic change. This is because the magnetic field arising from the upper portion of the crust ($0<z<\xi_3$) and that from the lower portion ($\xi_3<z<H$) nearly cancel each other. In the case of the T33 crack model, therefore, the magnetic field calculation is rather meaningless. Conversely, if no magnetic change is observed in association with some local but marked crustal uplift, the multiple T33 crack model could be a candidate for a

possible mechanism of the event.

5. The multiple T11 crack model

As for the surface displacement caused by a T11 crack, the symmetry breaks in a horizontally radial direction. The gravity and magnetic changes are also complicated. Two kind of regional stress fields are responsible for the opening of such cracks. In one field the horizontal shear stress is prevailing, which will give rise to vertical strike-slip fault. The other is the tensional field which will induce normal faulting.

Using the Galerkin vector given by MARUYAMA (1964), we can obtain Fourier transforms (4.3) and (4.5). They are summarized in Appendix A. The procedure to derive the surface displacement is the same as before. We denote the uplift, horizontal extension in the x and y direction by ΔH_{11}, ΔX_{11} and ΔY_{11} respectively. Fourier transforms of ΔH_{11}, ΔX_{11} and ΔY_{11} still contain ik_1^3 etc. We need final expressions for the surface displacement involving k only. This can be achieved by the repeated use of the formula (3.23). Results are shown as follows.

Uplift

$$\left.\begin{aligned}\Delta H_{11}=\frac{\Delta U}{2\pi}\Big[&\Big(2-\frac{1}{\alpha}\Big)\int_0^\infty U_1(k)J_0(kr)k\,dk\\&+\Big(\frac{1}{\alpha}-1\Big)\Big\{\Big(\frac{1}{r}-\frac{2x^2}{r^3}\Big)\int_0^\infty U_1(k)\,J_1(kr)\,dk+\frac{x^2}{r^2}\int_0^\infty U_1(k)J_0(kr)k\,dk\Big\}\\&-\Big(\frac{1}{r}-\frac{2x^2}{r^3}\Big)\int_0^\infty U_2(k)J_1(kr)k\,dk-\frac{x^2}{r^2}\int_0^\infty U_2(k)J_0(kr)k^2dk\Big]\end{aligned}\right\}\quad(5.1)$$

Horizontal extension in the x direction

$$\left.\begin{aligned}\Delta X_{11}=\frac{\Delta U}{2\pi}\Big[&\Big(\frac{1}{\alpha}-4\Big)\Big\{-\frac{x}{r}\int_0^\infty U_1(k)J_1(kr)k\,dk\Big\}\\&+\Big(2-\frac{1}{\alpha}\Big)\Big\{\Big(-\frac{6x}{r^3}+\frac{8x^3}{r^5}\Big)\int_0^\infty U_1(k)J_1(kr)\frac{dk}{k}-\frac{x^3}{r^3}\int_0^\infty U_1(k)J_1(kr)k\,dk\\&\qquad+\Big(\frac{3x}{r^2}-\frac{4x^3}{r^4}\Big)\int_0^\infty U_1(k)\,J_0(kr)\,dk\Big\}\\&+\Big(-\frac{6x}{r^3}+\frac{8x^3}{r^5}\Big)\int_0^\infty U_2(k)J_1(kr)\,dk-\frac{x^3}{r^3}\int_0^\infty U_2(k)J_1(kr)k^2dk\\&+\Big(\frac{3x}{r^2}-\frac{4x^3}{r^4}\Big)\int_0^\infty U_2(k)J_0(kr)k\,dk\Big]\end{aligned}\right\}\quad(5.2)$$

Horizontal extension in the y direction

$$\left.\begin{aligned}\Delta Y_{11}=\frac{\Delta U}{2\pi}\Big[&\Big(\frac{1}{\alpha}-2\Big)\Big\{\Big(-\frac{6y}{r^3}+\frac{8y^3}{r^5}\Big)\int_0^\infty U_1(k)J_1(kr)\frac{dk}{k}\\&-\frac{y^3}{r^3}\int_0^\infty U_1(k)J_1(kr)kdk+\Big(\frac{3y}{r^2}-\frac{4y^3}{r^4}\Big)\int_0^\infty U_1(k)J_0(kr)dk\Big\}\\&+\Big(-\frac{2y}{r^3}+\frac{8x^2y}{r^5}\Big)\int_0^\infty U_2(k)J_1(kr)dk-\frac{x^2y}{r^3}\int_0^\infty U_2(k)J_1(kr)k^2dk\\&+\Big(\frac{y}{r^2}-\frac{4x^2y}{r^4}\Big)\int_0^\infty U_2(k)J_0(kr)kdk\ \Big]\end{aligned}\right\}\quad(5.3)$$

where

$$\left.\begin{aligned}U_1(k)&=e^{-kD}Q_1(k)\\U_2(k)&=\frac{\sigma_z}{\sqrt{2\pi}}\exp\Big(-\frac{1}{2}\sigma_r{}^2k^2-\frac{1}{2}\frac{D^2}{\sigma_z{}^2}\Big)+(D-k\sigma_z{}^2)U_1(k)\end{aligned}\right\}\quad(5.4)$$

In the preceding two models the maximum uplift appears at $r=0$, so that Δh_0 is a useful measure for the moment intensity of strain nuclei. In the case of the multiple T11 crack model, however, the uplift at $r=0$ is not always the maximum one. Sometimes there are two humps along the x axis. The peak positions are different for each combination of model parameters $\{\sigma_r, \sigma_z, D\}$, which are not a simple function of x. We had better search numerically for the peak value $\Delta h_{\max}$ along the x axis, which may be used as a measure of ΔU.

Gravity change

We start by investigating the gravity field caused by a single T11 crack embedded at $(0, 0, \xi_3)$. As has been described before, G1 and G2 are given by definintion as

$$\text{G1}: \qquad \delta g_1=-\gamma\Delta h_p(x, y) \tag{5.5}$$

$$\text{G2}: \qquad \delta g_2=2\pi\rho G\Delta h_p(x, y) \tag{5.6}$$

where the uplift due to a T11 crack is given by

$$\begin{aligned}\Delta h_p(x, y)=\frac{\Delta U}{2\pi}\Big[&\Big(2-\frac{1}{\alpha}\Big)\frac{\xi_2}{R^3}+\Big(\frac{1}{\alpha}-1\Big)\Big\{\frac{1}{R(R+\xi_3)}-\frac{x^2(2R+\xi_3)}{R^3(R+\xi_3)^2}\Big\}\\&-2\xi_3\Big(\frac{1}{R^3}-\frac{2x^2}{R^5}\Big)\Big]\end{aligned}\tag{5.7}$$

G3 can be approximated by the gravity attraction of a point mass $\Delta U\,(\rho_0-\rho)$ which is identical to that of a T33 crack:

$$\text{G3}: \qquad \delta g_3 = \Delta U(\rho_0 - \rho) G \frac{\xi_3}{R^3} \tag{5.8}$$

Obviously this term is not in proportion to the surface uplift (5.7).

G4 can be represented by eq. (4.14), in which U_{33} should be replaced by U_{11}. Using $(div\ U_{11})^*$ in Appendix A, we obtain the Fourier transform of δg_4 as

$$\delta g_4^* = -\Delta U \rho G(1-\alpha)\left(2 - \frac{1}{\alpha} + \frac{1}{\alpha}\frac{k_1^2}{k^2}\right) e^{-k\xi_3} \tag{5.9}$$

Inversion of (5.9) gives rise to

$$\text{G4}: \qquad \delta g_4 = -\rho G \Delta U(1-\alpha)\left\{\left(2 - \frac{1}{\alpha}\right)\frac{\xi_3}{R^3} + \frac{1}{\alpha}\left(\frac{1}{R(R+\xi_3)} - \frac{x^2(2R+\xi_3)}{R^3(R+\xi_3)^2}\right)\right\} \tag{5.10}$$

In the T11 crack case, G4 is also not proportional to the uplift.

The gravity change associated with the multiple T11 crack model consists of Free-air (G1) and Bouguer (G2) terms in proportion to the uplift and non-proportional terms G3 and G4. The G3 term is equivalent to that of the multiple T33 crack model, which may be rewritten as

$$\delta G_3 = \Delta U(\rho_0 - \rho) G \int_0^\infty U_1(k) J_0(kr) k dk \tag{5.11}$$

wheae U_1 is already given in (5.4).

δG_4, the contribution from the density change, can be represented by

$$\delta G_4 = \int_0^\infty q(z') dz' \iint_{-\infty}^{\infty} \delta g_4(x-x', y-y', z') p(x', y') dx' dy' \tag{5.12}$$

in which we are to substitute (5.10) into δg_4 after rewriting the parameter ξ_3 with z'. With the aid of (3.6) and (5.9) we obtain

$$\delta G_4^* = -\Delta U \rho G(1-\alpha)\left(2 - \frac{1}{\alpha} + \frac{1}{\alpha}\frac{k_1^2}{k^2}\right) e^{-kD} Q_1(k) \tag{5.13}$$

Inverse transformation of eq. (5.13) gives

$$\begin{aligned}\delta G_4 = -\Delta U \rho G(1-\alpha)\Bigg[&\left(2 - \frac{1}{\alpha}\right)\int_0^\infty U_1(k) J_0(kr) k dk \\ &+ \frac{1}{\alpha}\left\{\left(\frac{1}{r} - \frac{2x^2}{r^3}\right)\int_0^\infty U_1(k) J_1(kr) dk + \frac{x^2}{r^2}\int_0^\infty U_1(k) J_0(kr) k dk\right\}\Bigg]\end{aligned} \tag{5.14}$$

The resultant gravity change δG_{11} is thus summarized as follows:

$$\delta G_{11}=(-\gamma+2\pi\rho G)\Delta H_{11}+\delta G_3+\delta G_4 \tag{5.15}$$

Magnetic change

Elementary piezomagnetic potentials due to the T11 type strain nucleus were obtained by SASAI (1980). Their Fourier transforms are reproduced in Appendix A. Applying the same method as in the preceding two models, we can derive magnetic potentials associated with the multiple T11 crack model. Final results are rather complicated because we have to replace powers of ik_1 and ik_2 with k by means of eq. (3.23):

$$W_{11}^x/C_{11}^x=\int_0^\infty\left[\left\{-\frac{x}{r}V_1^x(k,z)+\left(\frac{6x}{r^3}-\frac{8x^3}{r^5}+k^2\frac{x^3}{r^3}\right)V_2^x(k,z)\right\}J_1(kr)\right.$$
$$\left.-\left(\frac{3x}{r^2}-\frac{4x^3}{r^4}\right)V_2^x(k,z)J_0(kr)k\right]dk \tag{5.16a}$$

$$W_{11}^y/C_{11}^y=\int_0^\infty\left[\left\{-\frac{y}{r}V_1^y(k,z)+\left(\frac{6y}{r^3}-\frac{8y^3}{r^5}+k^2\frac{y^3}{r^5}\right)V_2^y(k,z)\right\}J_1(kr)\right.$$
$$\left.-\left(\frac{3y}{r^2}-\frac{4y^3}{r^4}\right)V_2^y(k,z)J_0(kr)k\right]dk \tag{5.16b}$$

$$W_{11}^z/C_{11}^z=\int_0^\infty\left[\left(\frac{1}{r}-\frac{2x^2}{r^3}\right)V_1^z(k,z)J_1(kr)\right.$$
$$\left.+\left\{\frac{x^2}{r^2}V_1^z(k,z)+V_2^z(k,z)\right\}J_0(kr)k\right]dk \tag{5.16c}$$

where

$$C_{11}^m=-\frac{1}{2}\mu\beta J_m\Delta U \qquad (m=x,y,z) \tag{5.17}$$

V_1^m and V_2^m are given in Appendix B. Again, the negative sign on the right of eq. (5.17) is adopted for the same reason as we have stated after eq. (4.21). Magnetic field components are also complicated, which will be found in Appendix C.

6. Examples

Shown in Fig. 4 are (a) uplift, (b) horizontal displacement, (c) gravity and (d) magnetic total field change associated with the multiple Mogi model for $D=1$ km, $\sigma_r=\sigma_z=0.5$ km and $\Delta h_0=10$ cm. These are profiles along the *N-S* meridian. Material properties of the medium and para-

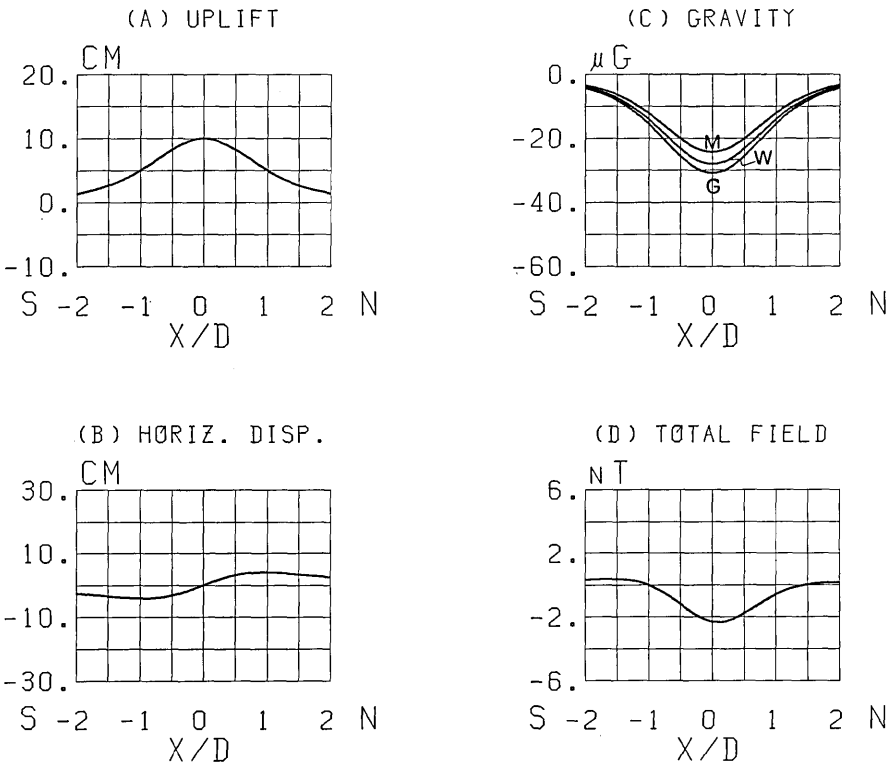

Fig. 4. Results along the N-S meridian for the multiple Mogi model with $D=1.0$ km, $\sigma_r=\sigma_z=0.5$ km and $\Delta h_0=10$ cm. (a) Uplift, (b) Horizontal displacement, (c) Gravity change: three curves indicate different kinds of crack-filling materials i.e. gas (G), water (W) and magma (M), and (d) Magnetic total intensity.

Table 1. Material properties of the elastomagnetic medium and parameters of the geomagnetic field.

Rigidity	μ	3.5×10^{11}	cgs
Poisson's ratio	ν	0.25	
Density	ρ	2.65	g/cc
Density of crack-filling materials	ρ_0		
Gas		0.0	g/cc
Water		1.0	g/cc
Magma		2.35	g/cc
Average magnetization	J	1.0×10^{-3}	emu/cc
Stress sensitivity	β	1.0×10^{-4}	bar^{-1}
Curie depth	H	15	km
Average magnetic dip	I_0	45	deg.

meters of the ambient geomagnetic field are summarized Table 1. Three curves in the gravity change correspond to three different materials filling cracks, i. e. gas (G), water (W) and magma (*M*). Since the detection capability of gravity change is at best $10\,\mu$ gal (TAJIMA 1975), it is difficult to distinguish each curve. In the case of an uplift of several tens centimeters, however, we may expect to specify the source material of the dilatant volume with the gravity data. As for the magnetic change, the overall decrease in the total intensity is predominant, which is reasonably anticipated from the piezomagnetic field of the single Mogi model.

Fig. 5 shows these quantities for model parameters $D=1.0$ km, $\sigma_r=\sigma_z=0.1$ km, 1 km and 10 km respectively. The gravity change is given for the water-saturated case only. Results for $\sigma_r=\sigma_z=0.1$ km are almost the same as those for the single Mogi model. In fact, we can confirm the multiple Mogi model practically coincides with the single Mogi model in case of $\sigma_r/D=\sigma_z/D=0.05$ or less.

Since the gravity change is proportional to the uplift, we have about

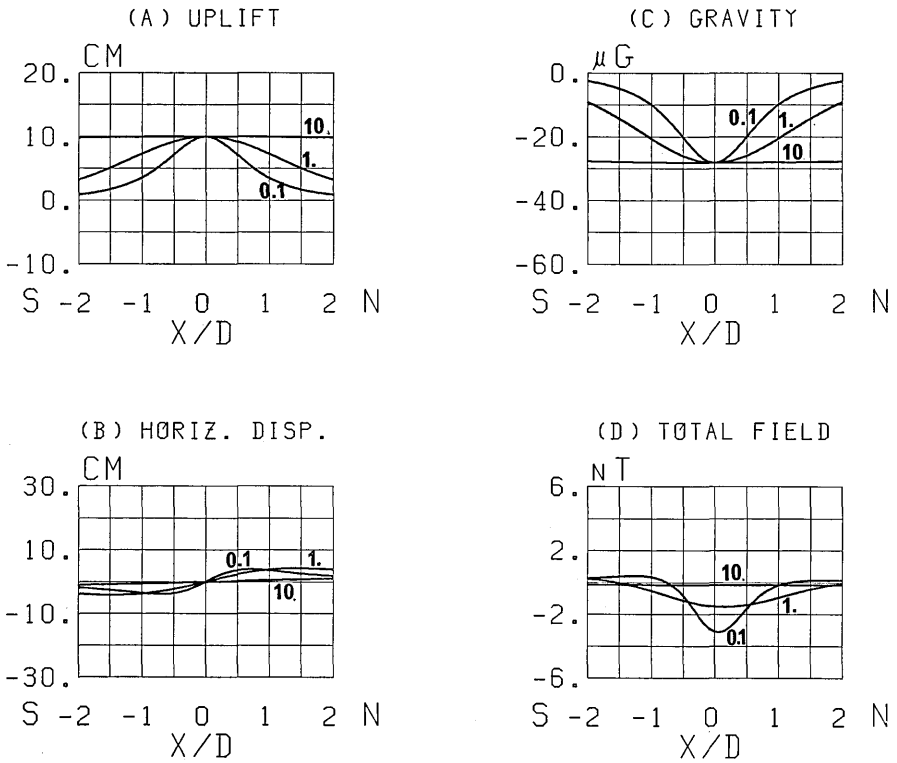

Fig. 5. The multiple Mogi model with $D=1.0$ km, $\Delta h_0=10$ cm, $\sigma_r=\sigma_z=0.1$, 1 and 10 km.

a 30 μ gal decrease against 10 cm uplift for any values of σ_r. On the other hand, the magnetic change diminishes as σ_r increases. Why do we meet such a phenomenon? The piezomagnetic potential due to the Mogi model is nothing but that of magnetic dipole placed at the dilation center, regardless of minor terms. Hence, in the multiple Mogi model, we are to calculate the field of dipoles distributed in Gaussian. With increasing σ_r, the crust behaves as a uniformly magnetized plate magnet with an infinite extent. A uniformly magnetized plate magnet of infinite extent produces no magnetic field outside it, no matter how intensely it is magnetized. Disappearance of the magnetic change with increasing σ_r is entirely attributed to this reason.

The intensity of the magnetic field is proportional to $\Delta h_0/D$. As the depth of the crack distribution center D increases, the magnetic field also decreases even for the same value of the given maximum uplift Δh_0. This is in contrast to the gravity change, which is directly proportional to Δh_0 and independent of D.

In Fig. 6 and Fig. 7 are depicted the surface displacements, gravity

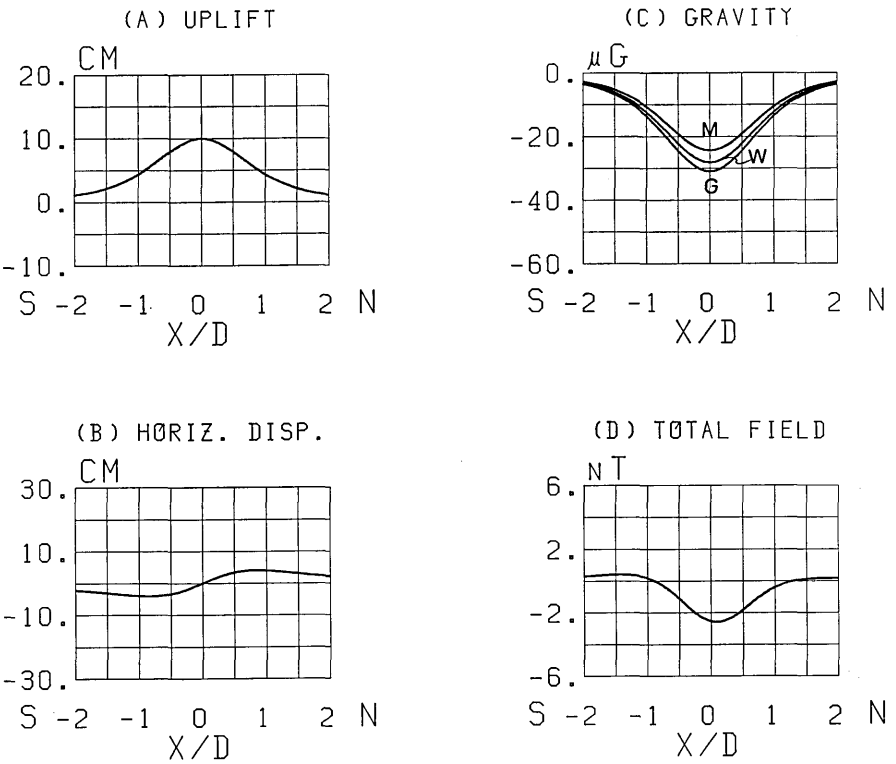

Fig. 6. The multiple Mogi model with D=1.0 km, Δh_0=10 cm, σ_r=0.5 km and σ_z=0.3 km.

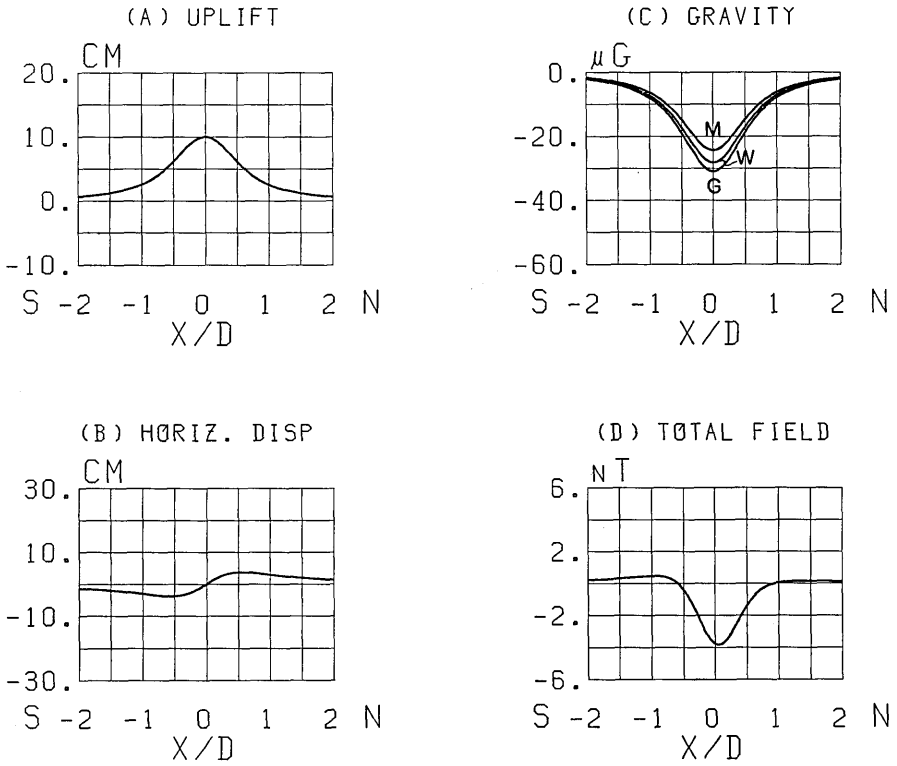

Fig. 7. The multiple Mogi model with D=1.0 km, Δh_0=10 cm, σ_r=0.3 km and σ_z=0.5 km.

and magnetic changes for the cases σ_r=0.5 km, σ_z=0.3 km and for σ_r= 0.3 km and σ_z=0.5 km respectively. The magnetic field is sensitive to the relative magnitude of σ_r and σ_z.

Next we will investigate the multiple T33 crack model. In Fig. 8 are shown the distortion-related quantities for model parameters D=1.0 km, $\sigma_r=\sigma_z$=0.5 km and Δh_0=10 cm, which are the same as in Fig. 4. The most outstanding feature is that the magnetic change is negligibly small for any combinations of parameters. The reason has already been stated in section 4. The surface displacements and gravity changes are very similar to those of the multiple Mogi model. It would be difficult to discriminate the two models with the displacement and gravity data alone. A slight but significant discrepancy between the two lies in the relative smallness of horizontal displacement in the T33 crack model.

Finally we will investigate the characteristics of the multiple T11 crack model. Fig. 9 shows the distortion-related quantities for the same model parameters as in Fig. 4 and 8. The results are remarkably different from the foregoing ones. First we find two humps in the uplift curve:

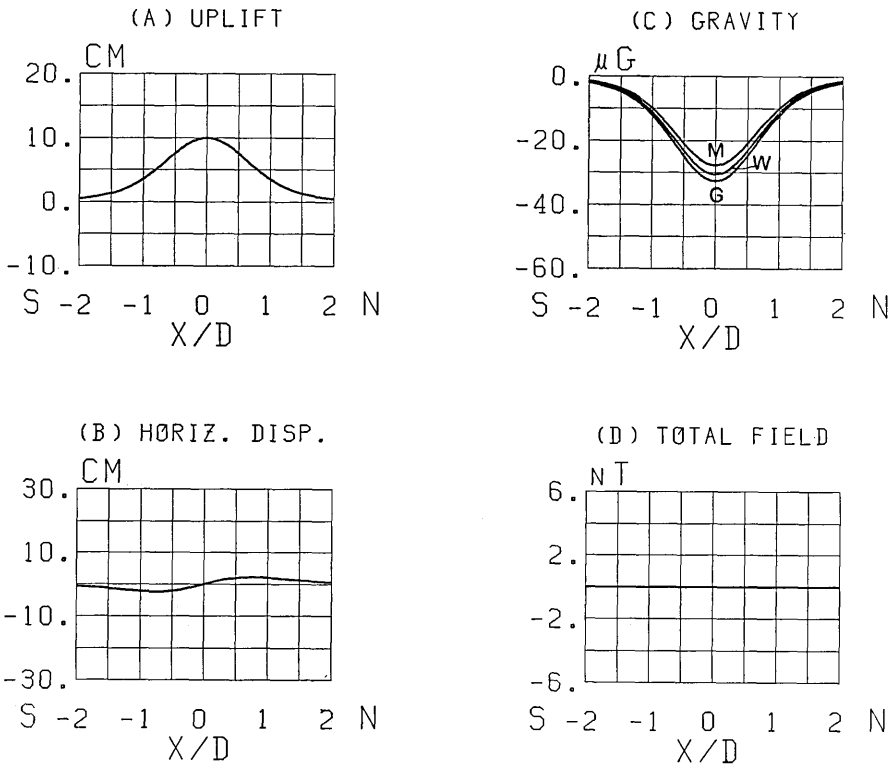

Fig. 8. The multiple T33 crack model with D=1.0 km, Δh_0=10 cm, $\sigma_r=\sigma_r$=0.5 km.

the origin above the center of crack distribution becomes a saddle point. In general the horizontal displacement prevails over the vertical one. The gravity change curves for three different crack-filling masses sufficiently deviate from each other even for a 10 cm upheaval, so that we can specify the source material. There appears a positive area in the total magnetic field on the southern slope of the uplift, although the negative area on the north is dominant.

Augmentation of gravity change is explained as follows: The maximum uplift $\Delta h_{\max}$ plays the role of a measure for the total crack volume in the present calculation. Since a single T11 crack is less capable of producing the surface uplift, much more crack volume is required to attain a certain amount of upheaval as compared to the spherical or T33 cracks. Hence the G3 term becomes dominant, which reflects the material density within cracks directly.

For the multiple T11 crack model, asymmetry appears in a horizontal direction. Profiles along a line parallel to the crack orientation are given in Fig. 10. The direction of the magnetic north is also deflected away

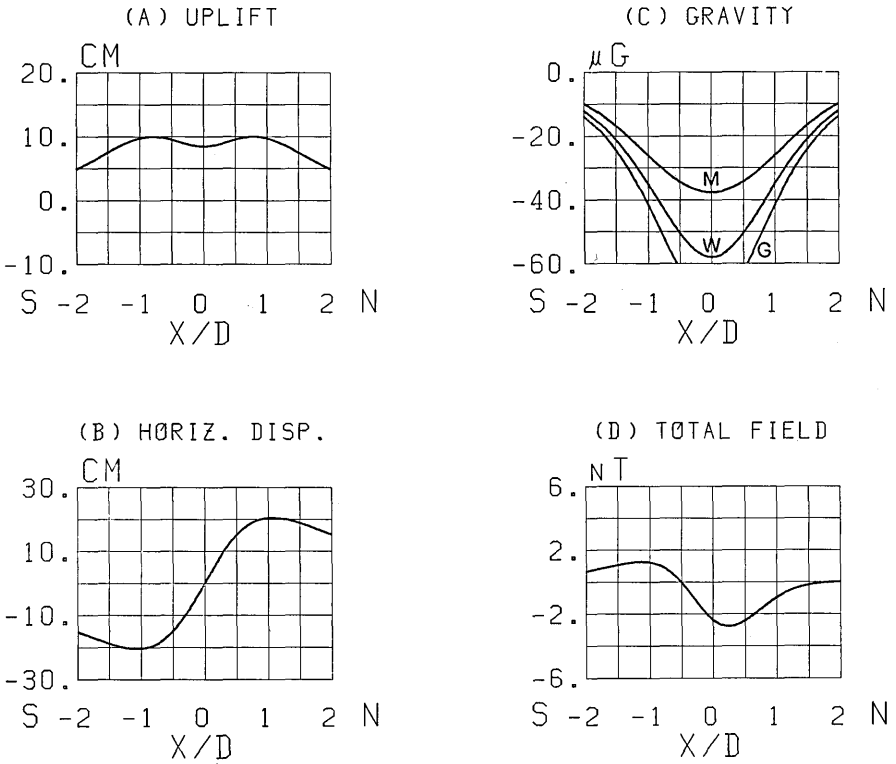

Fig. 9. The multiple T11 crack model with D=1.0 km, Δh_0=10 cm, $\sigma_r=\sigma_z$=0.5 km. The crack orientation is perpendicular to the profile.

by 90°. They are N-S profiles of the T22 type cracks. Along such a meridian, the maximum uplift is at the col and the horizontal displacement becomes much less than that in Fig. 9(b). The gravity change is large, while the magnetic field takes on a weak negative value throughout. Adding the magnetic change in Fig. 9 (d) and Fig. 10 (d) (strictly speaking, together with a negligible amount of contribution in Fig. 8 (d)), we obtain the overall negative change due to the multiple Mogi model in Fig. 4 (d). This can be recognized from the nature of the center of dilatation as has been discussed in section 2.

In Fig. 11 are shown N-S profiles for $\sigma_r=\sigma_z$=0.1 km, 1 km and 10 km, respectively. For small σ_r and σ_z, the saddle-like deformation of the surface is intensified. Even a subsidense occurs at the origin. This is well-known for a single T11-crack. In fact, we find the vertical displacement for $\sigma_r=\sigma_z$=0.1 km is coincident with MARUYAMA's (1964) result for a T11 strain nucleus. On the other hand, this feature disappears for $\sigma_r=\sigma_z$=1.0 km. It is ascertained that around $\sigma_r=\sigma_z$=0.6 km the two humps

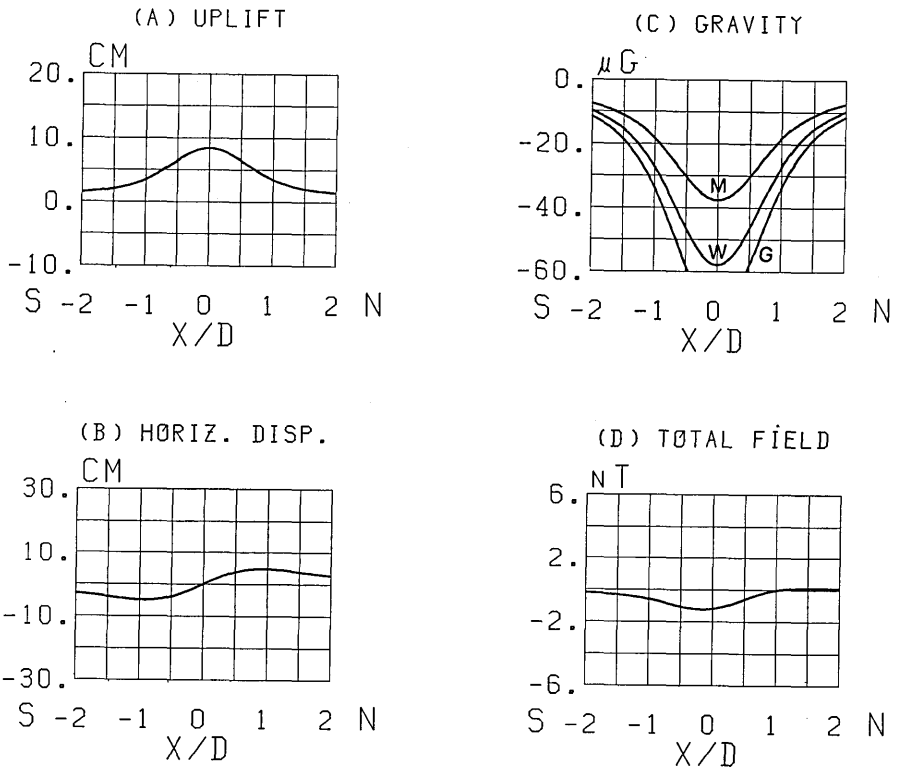

Fig. 10. The multiple T11 crack model with the same parameters as in Fig. 9. The crack orientation is parallel to the profile.

vanish and the plateau-like upheaval emerges instead. A similar feature of the magnetic change to the multiple Mogi model is observed wherein the total field diminishes as the σ_r increases. This is ascribed for the same reason as given before.

In Figs. 12 and 13 are shown profiles for the cases $\sigma_r=0.5$ km, $\sigma_z=0.3$ km and for $\sigma_r=0.3$ km and $\sigma_z=0.5$ km, respectively. Generally the gravity and magnetic changes are intensified when $\sigma_r<\sigma_z$.

There are two outstanding features in the gravity change: (i) the peak position of the maximum gravity change does not always coincide with that of the uplift. In Fig. 9 (c) we find the maximum change in gravity appears at the origin in spite of two humps in the uplift curve. For the $\sigma_r=\sigma_z=0.1$ km case in Figs. 11 (a) and (c), two peaks exist in both the uplift annd gravity, but their positions are clearly separated. Moreover, peak positions of gravity change are slightly different for the three kinds of crack materials. (ii) We may expect an extremely large value in the gravity change rate. The highest expected rate in the multiple

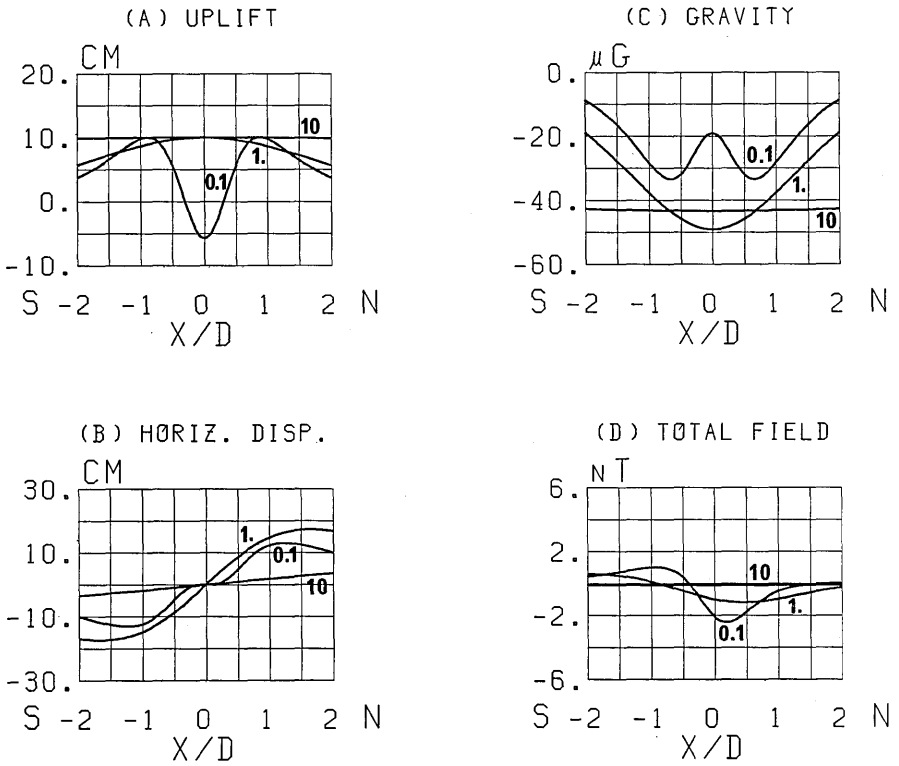

Fig. 11. The multiple T11 crack model with D=1.0 km, Δh_0=10 cm, $\sigma_r=\sigma_z$=0.1 km, 1 km and 10 km, respectively.

Mogi model is the free air rate (i. e. $\rho_0=0$ in eq. (3.31)). For the multiple T11 crack model, however, the rate is a function of the observation site. In Fig. 9 (c), we see that the gravity change rate at the origin amounts to $-7\,\mu$gal/cm for dry dilatancy (i. e. more than twice the free-air rate). Unsual gravity changes will be a useful constraint on the multiple T11 crack model.

All these examples indicate that the magnetic change is observable only when the dilatant region is shallow and localized. A large-scale crustal dilatancy is, however, somewhat unreal. The present study tells us that magnetic measurement is promising to detect the onset of dilatancy at locked portions of a fault if it occurs prior to the rupture.

7. Application to volcanology

We have presented here a kinematic model for crustal dilatancy. The term "kinematic" implies that we give a priori the amount of the

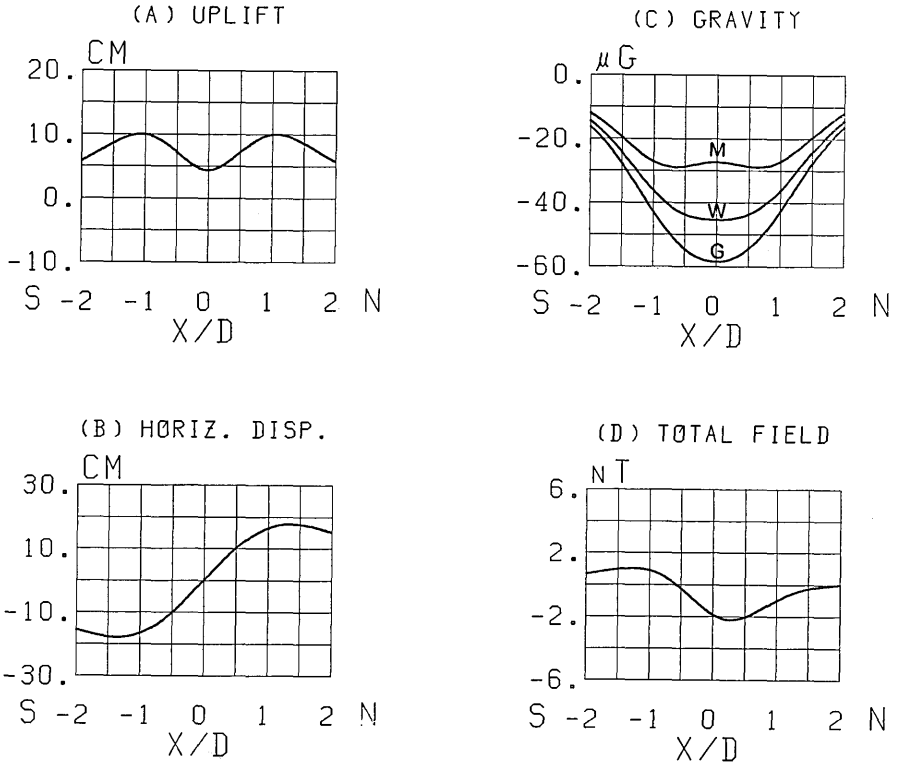

Fig. 12. The multiple T11 crack model with D=1.0 km, Δh_0=10 cm, σ_r=0.5 km and σ_z=0.3 km.

source deformation regardless of its physical mechanism. Three types of dilatant deformation processes are proposed to cause volumetric increase of crustal materials under shear stresses, namely a) sand, b) joint and c) microcrack dilatancy (NUR 1975). In the case of the sand dilatancy the rigid body rotation of granular masses plays the major role: the density and magnetization changes would be different from those we have considered in this paper. We prefer the joint and microcrack dilatancies in applying our model. There still remains a discrepancy: cracks formed by the *in situ* rock dilatancy are not always sustained by crack-filling materials, while dislocations in our model should naturally be maintained by some internal pressure. In other words, the present model is the most suitable for the case where tensile cracks are produced by forced injection of some pressurized substances.

HILL (1977) proposed a generating mechanism of earthquake swarms in volcanic regions: a number of tensile cracks filled with magma open in some preferred direction under the regional stress field, and shear

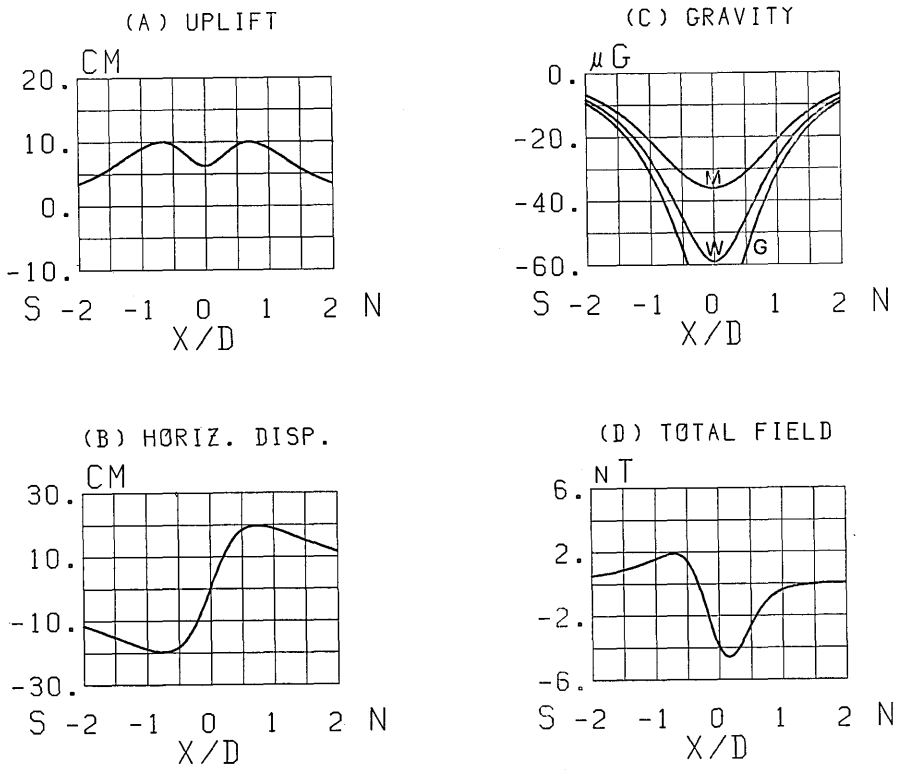

Fig. 13. The multiple T11 crack model with $D=1.0$ km, $\Delta h_0=10$ cm, $\sigma_r=0.3$ km and $\sigma_z=0.5$ km.

dislocations develop so as to connect these cracks. If the spacing of dykes is sparce, we may employ the multiple tension crack model as an approximation to Hill's mechanism. We must be carefull, however, to apply the model to the near-field data, since the mutual coupling of fluid inclusions should certainly alter the results hitherto described in this paper.

The multiple tension-crack model works as a simulator for the magma reservoir. In the previous section we found the multiple Mogi model with small σ_r ane σ_z coincides with the single Mogi model, which is a useful tool in volcanology. By analogy with the single Mogi model, the multiple model can be regarded as an assemblage of small magma pockets. Such a magma reservoir may have some spatial extent and different aspect ratio in contrast to the limitation originally imposed on the Mogi model.

FISKE and KINOSHITA (1969) suggested the aggregate of sills and dykes as the reservoir beneath the Kilauea Volcano, Hawaii. The multiple

Mogi model can be viewed as a cluster of tensile cracks oriented in every direction: it seems suitable as a first-order approximation for the Fiske and Kinoshita's model. A merit of the multiple tension-crack model applied to the magma reservoir is that magma is scattered within rigid host rocks: the firm framework is built in within the reservoir. We need not worry about the large-scale collapse of the vacancy after the eruption, which enevitably accompany traditional reservoir models with a large cavity.

As for the multiple Mogi model there are two other candidates for its physical entity. One is the thermal expansion. Its mechanical distortion can be calculated by replacing the center of dilatation whose intensity is proportional to the increased temperature. The temperature increase with a spatially Gaussian distribution will cause exactly the same mechanical effect as the multiple Mogi model. The other is a model for dacite volcanism. WATANABE (1984) presented a bubble growth model in the dacite magma supersaturated with volatiles. He ascribed it to the driving force of the cript-dome formation at Usu Volcano, Japan. Such a force source can be again simulated by the multiple Mogi model with appropriate σ_r and σ_z.

The multiple tension-crack model is thus useful for describing volcanic phenomena. We should, however, take into account changes in the material properties due to the high temperature. In particular, thermal demagnetization surely affects the magnetic field. We have to subtract the contribution of the hot region from the solution given in this paper. This can be successfully achieved with the aid of the surface integral representation of the tectonomagnetic field (SASAI 1983).

The multiple tension-crack model is now applied to the anomalous crustal uplift associated with the Matsushiro swarm earthquakes, the result of which will be reported elsewhere.

Acknowledgements

I am deeply indebted to Professor Yukio Hagiwara, who motivated the present work and discussed various aspects of the problem. Applicability of the present model to volcanology was suggested through discussions and advice from Tsutomu Miyazaki, Munehisa Sawada, Tsuneomi Kagiyama and Ken'ichiro Yamashina, whom I acknowledge sincerely.

Appendix A Fourier transforms

All the Fourier transforms referred to in this study are summarized. Some of them are reproduced from SASAI (1979, 1980).

A 1: Displacement field of a T33 crack at $(0, 0, \xi_3)$

$$\frac{4\pi}{\Delta U}U_{33}^{x*}=\left\{-\alpha ik_1\zeta_1+(1-\alpha)\frac{ik_1}{k}\right\}e^{-k\zeta_1}$$
$$+\left\{(\alpha-1)\frac{ik_1}{k}+(\alpha-2)ik_1\xi_3+(\alpha ik_1+2\alpha ik_1k\xi_3)z\right\}e^{-k\zeta_2} \tag{A.1}$$

$$\frac{4\pi}{\Delta U}U_{33}^{y*}=\left\{-\alpha ik_2\zeta_1+(1-\alpha)\frac{ik_2}{k}\right\}e^{-k\zeta_1}$$
$$+\left\{(\alpha-1)\frac{ik_2}{k}+(\alpha-2)ik_2\xi_3+(\alpha ik_2+2\alpha ik_2k\xi_3)z\right\}e^{-k\zeta_2} \tag{A.2}$$

$$\frac{4\pi}{\Delta U}U_{33}^{z*}=\pm\left\{\{(1+\alpha)k\zeta_1+1\}e^{-k\zeta_1}+\{-1+(\alpha-1)k\xi_3+(k-\alpha k^2\xi_3)z\}e^{-k\zeta_2}\right. \tag{A.3}$$

$$\frac{4\pi}{\Delta U}(div\ U_{33})^*=2(\alpha-1)ke^{-k\zeta_1}+2\{(1+\alpha)k+2k^2\xi_3\}e^{-k\zeta_2} \tag{A.4}$$

where the double sign corresponds to $z\gtrless\xi_3$,

and
$$\zeta_1=|z-\xi_3|,\quad \zeta_2=z+\xi_3. \tag{A.5}$$

$$\frac{4\pi}{\Delta U}\Delta h_p{}^*=2(1+k\xi_3)e^{-k\xi_3} \tag{A.6}$$

$$\frac{4\pi}{\Delta U}\Delta x_p{}^*=-2ik_1\xi_3e^{-k\xi_3} \tag{A.7}$$

$$\frac{4\pi}{\Delta U}\Delta y_p{}^*=-2ik_2\xi_3e^{-k\xi_3} \tag{A.8}$$

A2: Displacement field of a T11 crack at $(0, 0, \xi_3)$

$$\frac{4\pi}{\Delta U}U_{11}^{x*}=\left\{\alpha\frac{ik_1{}^3}{k^3}+\alpha\frac{ik_1{}^3}{k^2}\zeta_1-(1+2\alpha)\frac{ik_1}{k}\right\}e^{-k\zeta_1}$$
$$+\left\{\alpha\frac{ik_1{}^3}{k^3}+\alpha\frac{ik_1{}^3}{k^2}\zeta_2-(1+2\alpha)\frac{ik_1}{k}\right\}e^{-k\zeta_2}$$
$$+2\left\{(\alpha-1)\left(2-\frac{1}{\alpha}\right)\frac{ik_1}{k}-\frac{(1-\alpha)^2}{\alpha}\frac{ik_1{}^3}{k^3}+(1-\alpha)\xi_3\frac{ik_1{}^3}{k^2}\right\}e^{-k\zeta_2}$$
$$+2\left\{(2\alpha-1)ik_1+(1-\alpha)\frac{ik_1{}^3}{k^2}-\alpha\xi_3\frac{ik_1{}^3}{k}\right\}ze^{-k\zeta_2} \tag{A.9}$$

$$\frac{4\pi}{\Delta U}U_{11}^{y*}=\left\{(1-\alpha)\frac{ik_2}{k}-\alpha\frac{ik_2{}^3}{k^3}+\alpha\frac{ik_1{}^2k_2}{k^2}\zeta_1\right\}e^{-k\zeta_1}$$

$$+\left\{(1-\alpha)\frac{ik_2}{k}-\alpha\frac{ik_2^3}{k^3}+\alpha\frac{ik_1^2k_2}{k^2}\zeta_2\right\}e^{-k\zeta_2}$$

$$+2\left\{(\alpha-1)\frac{ik_2}{k}+\frac{(1-\alpha)^2}{\alpha}\frac{ik_2^3}{k^3}+(1-\alpha)\xi_3\frac{ik_1^2k_2}{k^2}\right\}e^{-k\zeta_2}$$

$$+2\left\{\alpha ik_2+(\alpha-1)\frac{ik_2^3}{k^2}-\alpha\xi_3\frac{ik_1^2k_2}{k}\right\}ze^{-k\zeta_2} \qquad \text{(A.10)}$$

$$\frac{4\pi}{\Delta U}U_{11}^{z*}=\mp\left\{(1-2\alpha)+\alpha\frac{k_1^2}{k}\zeta_1\right\}e^{-k\zeta_1}-\left\{(1-2\alpha)+\alpha\frac{k_1^2}{k}\zeta_2\right\}e^{-k\zeta_2}$$

$$+2\left\{-\left(2-\frac{1}{\alpha}\right)+\left(1-\frac{1}{\alpha}\right)\frac{k_1^2}{k^2}+\frac{k_1^2}{k}\zeta_3\right\}e^{-k\zeta_2}$$

$$+2\left\{(1-2\alpha)k+(\alpha-1)\frac{k_1^2}{k}+\alpha\xi_3k_1^2\right\}ze^{-k\zeta_2} \qquad \text{(A.11)}$$

$$\frac{4\pi}{\Delta U}(div\,U_{11})^*=2(1-\alpha)\frac{k_1^2}{k}e^{-k\zeta_1}+2(1-\alpha)\frac{k_1^2}{k}e^{-k\zeta_2}$$

$$+4(1-\alpha)\left\{\left(2-\frac{1}{\alpha}\right)k+\left(\frac{1}{\alpha}-1\right)\frac{k_1^2}{k}-\xi_3k_1^2\right\}e^{-k\zeta_2} \qquad \text{(A.12)}$$

$$\frac{4\pi}{\Delta U}\Delta h_p^*=2\left\{2-\frac{1}{\alpha}+\left(\frac{1}{\alpha}-1\right)\frac{k_1^2}{k^2}-\xi_3\frac{k_1^2}{k}\right\}e^{-k\xi_3} \qquad \text{(A.13)}$$

$$\frac{4\pi}{\Delta U}\Delta x_p^*=2\left\{\left(\frac{1}{\alpha}-4\right)\frac{ik_1}{k}+\left(2-\frac{1}{\alpha}\right)\frac{ik_1^3}{k^3}+\xi_3\frac{ik_1^3}{k^2}\right\}e^{-k\xi_3} \qquad \text{(A.14)}$$

$$\frac{4\pi}{\Delta U}\Delta y_p^*=2\left\{\left(\frac{1}{\alpha}-2\right)\frac{ik_2^3}{k^3}+\xi_3\frac{ik_1^2k_2}{k^2}\right\}e^{-k\xi_3} \qquad \text{(A.15)}$$

A3: Piezomagnetic potential due to the Mogi model

$$\frac{w_{00}^{z*}}{C_{00}^z}=-\frac{\mu}{2(\lambda+\mu)}\frac{ik_1}{k}(e^{-kD_1}-e^{-kD_3})-3Hik_1e^{-kD_3}$$

$$+\begin{cases}0 & (H<\xi_3)\\ -\dfrac{3}{2}\dfrac{ik_1}{k}(e^{-kD_1}-e^{-kD_2}) & (0<\xi_3<H)\end{cases} \qquad \text{(A.16)}$$

$$\frac{w_{00}^{z*}}{C_{00}^z}=-\frac{\mu}{2(\lambda+\mu)}(e^{-kD_1}-e^{-kD_3})+3Hke^{-kD_3}$$

$$+\begin{cases}0 & (H<\xi_3)\\ \dfrac{3}{2}(e^{-kD_1}-e^{-kD_2}) & (0<\xi_3<H)\end{cases} \qquad \text{(A.17)}$$

where D_1, D_2 and D_3 are already given in (3.33).

A4: Piezomagnetic potential due to a T33 strain nucleus

$$\frac{w_{33}^{z*}}{C_{33}^{z}}=\left\{\frac{1-4\alpha}{2}\frac{ik_1}{k}+(1-\alpha)ik_1\xi_3\right\}(e^{-kD_1}-e^{-kD_3})$$
$$+(3\alpha ik_1+6\alpha\xi_3 ik_1k)He^{-kD_3}$$
$$+\begin{cases}(\alpha-1)ik_1He^{-kD_1} & (H<\xi_3)\\ -\dfrac{1-4\alpha}{2}\dfrac{ik_1}{k}(e^{-kD_1}-e^{-kD_2}) & \\ +(\alpha-1)ik_1\xi_3e^{-kD_1}-3\alpha ik_1(H-\xi_3)e^{-kD_2} & (0<\xi_3<H)\end{cases} \tag{A.18}$$

$$w_{33}^{y*}(k_1, k_2)=w_{33}^{z*}(k_2, k_1) \tag{A.19}$$

$$\frac{w_{33}^{z*}}{C_{33}^{z}}=\left\{\frac{1+2\alpha}{2}+(1-\alpha)k\xi_3\right\}(e^{-kD_1}-e^{-kD_3})+(-3\alpha k-6\alpha\xi_3k^2)He^{-kD_3}$$
$$+\begin{cases}(\alpha-1)kHe^{-kD_1} & (H<\xi_3)\\ -\dfrac{1+2\alpha}{2}(e^{-kD_1}-e^{-kD_3}) & \\ +(\alpha-1)k\xi_3e^{-kD_1}+3\alpha k(H-\xi_3)e^{-kD_2} & (0<\xi_3<H)\end{cases} \tag{A.20}$$

A5: Piezomagnetic potential due to a T11 strain nucleus

$$\frac{w_{11}^{z*}}{C_{11}^{z}}=\left\{\frac{3}{2}\frac{ik_1}{k}+\frac{(2-\alpha)(4\alpha-1)}{2\alpha}\frac{ik_1k_2^2}{k^3}+(\alpha-1)\frac{ik_1^3}{k^2}\xi_3\right\}(e^{-kD_1}-e^{-kD_3})$$
$$+\left\{9\alpha\frac{ik_1^3}{k^2}-6(1-2\alpha)\frac{ik_1k_2^2}{k^2}-6\alpha\frac{ik_1^3}{k}\xi_3\right\}He^{-kD_3}$$
$$+\begin{cases}(1-\alpha)\dfrac{ik_1^3}{k^2}He^{-kD_1} & (H<\xi_3)\\ \left\{\dfrac{1-4\alpha}{2}\dfrac{ik_1^3}{k^3}+6\alpha\dfrac{ik_1}{k}\right\}(e^{-kD_1}-e^{-kD_2}) & \\ +(1-\alpha)\dfrac{ik_1^3}{k^2}\xi_3e^{-kD_1}+3\alpha\dfrac{ik_1^3}{k^2}(H-\xi_3)e^{-kD_2} & (0<\xi_3<H)\end{cases} \tag{A.21}$$

$$\frac{w_{11}^{y*}}{C_{11}^{y}}=\left\{-\frac{3}{2}\frac{ik_1^2k_2}{k^3}+\frac{(2\alpha-1)(1-\alpha)}{\alpha}\frac{ik_2^3}{k^3}+(\alpha-1)\frac{ik_1^2k_2}{k^2}\xi_3\right\}(e^{-kD_1}-e^{-kD_3})$$
$$+\left\{9\alpha\frac{ik_1^2k_2}{k^2}-6(1-2\alpha)\frac{ik_2^3}{k^2}-6\alpha\frac{ik_1^2k_2}{k}\xi_3\right\}He^{-kD_3}$$

$$+\begin{cases}(1-\alpha)\dfrac{ik_1^3}{k^2}He^{-kD_1} & (H<\xi_3)\\ \left(\dfrac{1-4\alpha}{2}\dfrac{ik_1^3}{k^3}+6\alpha\dfrac{ik_1}{k}\right)(e^{-kD_1}-e^{-kD_2}) & \\ +(1-\alpha)\dfrac{ik_1^3}{k^2}\xi_3e^{-kD_1}+3\alpha\dfrac{ik_1^3}{k^2}(H-\xi_3)e^{-kD_2} & (0<\xi_3<H)\end{cases} \qquad (A.22)$$

$$\frac{w_{11}^{z*}}{C_{11}^z}=\left\{\frac{3}{2}(1-2\alpha)\frac{k_1^2}{k^2}+\frac{(2\alpha-1)(1-\alpha)}{\alpha}\frac{k_2^2}{k^2}+(\alpha-1)\frac{k_1^2}{k}\xi_3\right\}(e^{-kD_1}-e^{-kD_3})$$
$$+\left\{-9\alpha\frac{k_1^2}{k}+6(1-2\alpha)\frac{k_2^2}{k}+6\alpha k_1^2\xi_3\right\}He^{-kD_3}$$
$$+\begin{cases}(1-\alpha)\dfrac{k_1^2}{k}He^{-kD_1} & (H<\xi_3)\\ \left\{\dfrac{2\alpha-5}{2}\dfrac{k_1^2}{k^2}+3(1-2\alpha)\right\}(e^{-kD_1}-e^{-kD_2}) & \\ +(1-\alpha)\dfrac{k_1^2}{k}\xi_3e^{-kD_1}-3\alpha\dfrac{k_1^2}{k}(H-\xi_3)e^{-kD_2} & (0<\xi_3<H)\end{cases} \qquad (A.23)$$

Appendix B Weight functions for magnetic potentials

$\overline{W}_{00}^z$ and $\overline{W}_{00}^z$ in eq. (3.34), $\overline{W}_{33}^z$ and $\overline{W}_{33}^z$ in eq. (4.20) and V_1^x, V_2^x, V_1^y, V_2^y, V_1^z and V_2^z in eq. (5.16) are summarized. They consist of R functions arising from integrals of a form $\int_0^A z'^l q(z')dz'$ ($l=0$ or 1, $A=H$ or ∞). R functions are listed separately.

B1: The multiple Mogi model

$$\overline{W}_{00}^z(k,z)=-\frac{\mu}{2(\lambda+\mu)}\frac{1}{k}R_1-3HR_3-\frac{3}{2}\frac{1}{k}R_6 \qquad (B.1)$$

$$\overline{W}_{00}^z(k,z)=-\frac{\mu}{2(\lambda+\mu)}R_1+3HkR_3+\frac{3}{2}R_6 \qquad (B.2)$$

B2: The multiple T33 crack model

$$\overline{W}_{33}^z(k,z)=\frac{1-4\alpha}{2}\frac{1}{k}(R_1-R_6)+(1-\alpha)(R_2-HR_5-R_7)$$
$$+3\alpha(HR_3+2HkR_4-HR_8+R_9) \qquad (B.3)$$

$$\overline{W}^{z}_{33}(k, z)=\frac{1+2\alpha}{2}(R_1-R_6)+(1-\alpha)k(R_2-HR_5-R_7)$$
$$+3\alpha k(-HR_3-2HkR_4+HR_8-R_9) \tag{B.4}$$

B3: *The multiple T11 crack model*

$$V_1{}^{x}(k, z)=\left\{-\frac{1-6\alpha+2\alpha^2}{\alpha}R_1+6\alpha R_6-6(1-2\alpha)HR_3k\right\}k \tag{B.5}$$

$$V_2{}^{x}(k, z)=\frac{4\alpha-1}{2}\left(\frac{2-\alpha}{\alpha}R_1+R_6\right)+(1-\alpha)(R_2-HR_5)$$
$$-3(2-\alpha)HR_3+3\alpha(2HR_4k-HR_8+R_9) \tag{B.6}$$

$$V_1{}^{y}(k, z)=\left\{-\frac{3}{2}R_1+(1-\alpha)(-R_2+HR_5+R_7)k+\frac{8\alpha-5}{2}R_6\right.$$
$$\left.+3\alpha(3HR_3-2HR_4k+HR_8-R_9)k\right\}k \tag{B.7}$$

$$V_2{}^{y}(k, z)=-V_2{}^{x}(k, z) \tag{B.8}$$

$$V_1{}^{z}(k, z)=\frac{(1-2\alpha)(2+\alpha)}{2}R_1+(1-\alpha)(-R_2+HR_5+R_7)k-3(2-\alpha)HR_3k$$
$$+\frac{2\alpha-5}{2}R_6+3\alpha(2HR_4k-HR_8+R_9)k \tag{B.9}$$

$$V_2{}^{z}(k, z)=\frac{(2\alpha-1)(1-\alpha)}{\alpha}R_1+6(1-2\alpha)HR_3k+3(1-2\alpha)R_6 \tag{B.10}$$

B4: *R functions*

$$R_1(k, z)=Q_1(k)(e^{-kD_1}-e^{-kD_3}) \tag{B.11}$$

$$R_2(k, z)=\frac{\sigma_z}{\sqrt{2\pi}}\exp\left(-\frac{1}{2}\sigma_r{}^2k^2+zk-\frac{D^2}{2\sigma_z{}^2}\right)(1-e^{-2Hk})+(D-k\sigma_z{}^2)R_1(k, z) \tag{B.12}$$

$$R_3(k, z)=Q_1(k)e^{-kD_3} \tag{B.13}$$

$$R_4(k, z)=\frac{\sigma_z}{\sqrt{2\pi}}\exp\left\{-\frac{1}{2}\sigma_r{}^2k^2+(z-2H)k-\frac{D^2}{2\sigma_z{}^2}\right\}+(D-k\sigma_z{}^2)R_3(k, z) \tag{B.14}$$

$$R_5(k, z)=Q_2(k)e^{-kD_1} \tag{B.15}$$

$$R_6(k, z)=Q_{12}(k)e^{-kD_1}-Q_{34}(k)e^{-kD_2} \tag{B.16}$$

$$R_7(k,z)=\frac{\sigma_z}{\sqrt{2\pi}}\exp\left(-\frac{1}{2}\sigma_r^2k^2+zk\right)\left\{\exp\left(-\frac{D^2}{2\sigma_z^2}\right)-\exp\left(-Hk-\frac{(H-D)^2}{2\sigma_z^2}\right)\right\}$$
$$+(D-k\sigma_z^2)Q_{12}(k)e^{-kD_1} \tag{B.17}$$

$$R_8(k,z)=Q_{34}(k)e^{-kD_2} \tag{B.18}$$

$$R_9(k,z)=\frac{\sigma_z}{\sqrt{2\pi}}\exp\left(-\frac{1}{2}\sigma_r^2k^2+zk\right)\left\{\exp\left(-2Hk-\frac{D^2}{2\sigma_z^2}\right)\right.$$
$$\left.-\exp\left(-Hk-\frac{(H-D)^2}{2\sigma_z^2}\right)\right\}+(D+\sigma_z^2k)R_8(k,z) \tag{B.19}$$

where

$$Q_1(k)=\exp\left\{-\frac{1}{2}(\sigma_r^2-\sigma_z^2)k^2\right\}\Phi(x_1) \tag{B.20}$$

$$Q_2(k)=\exp\left\{-\frac{1}{2}(\sigma_r^2-\sigma_z^2)k^2\right\}\Phi(x_2) \tag{B.21}$$

$$Q_{12}(k)=Q_1(k)-Q_2(k) \tag{B.22}$$

$$Q_{34}(k)=\exp\left\{-\frac{1}{2}(\sigma_r^2-\sigma_z^2)k^2\right\}\{\Phi(x_3)-\Phi(x_4)\} \tag{B.23}$$

$$x_1=\frac{-D+\sigma_z^2k}{\sqrt{2}\,\sigma_z},\quad x_2=\frac{H-D+\sigma_z^2k}{\sqrt{2}\,\sigma_z},\quad x_3=\frac{-D-\sigma_z^2k}{\sqrt{2}\,\sigma_z},\quad x_4=\frac{H-D-\sigma_z^2k}{\sqrt{2}\,\sigma_z} \tag{B.24}$$

$\Phi(x)$ is defined by eq. (3.10).

In the case that $\sigma_r<\sigma_z$, the expressions (B. 20)—(B. 23) are inadequate, since the exponential terms become divergent. Instead we had better use the following formulas for large k.

$$Q_1(k)=\exp\left\{-\frac{1}{2}\left(\sigma_r^2k^2+\frac{D^2}{\sigma_z^2}\right)\right\}\Psi(x_1) \tag{B.25}$$

$$Q_2(k)=\exp\left\{-\frac{1}{2}\left(\sigma_r^2k^2+2Hk+\frac{(H-D)^2}{\sigma_z^2}\right)\right\}\Psi(x_2) \tag{B.26}$$

$$Q_{12}(k)=Q_1(k)-Q_2(k) \tag{B.27}$$

$$Q_{34}(k)=\exp\left\{-\frac{1}{2}\left(\sigma_r^2k^2+\frac{D^2}{\sigma_z^2}\right)\right\}\Psi(x_3)$$
$$-\exp\left\{-\frac{1}{2}\left(\sigma_r^2k^2-2Hk+\frac{(H-D)^2}{\sigma_z^2}\right)\right\}\Psi(x_4) \tag{B.28}$$

where

$$\Psi(x)=e^{x^2}\Phi(x) \tag{B.29}$$

Useful approximation formulas for *erfc* (x) involved in $\Phi(x)$ and e^{x^2} *erfc* (x) in $\Psi(x)$ are found in HASTINGS (1955).

Appendix C Magnetic field of the multiple T11 crack model

$$\frac{\Delta X^x_{11}}{C^x_{11}}=\int_0^\infty\left(\frac{1}{2}V_1{}^x-\frac{3}{8}k^2V_2{}^x\right)J_0(kr)kdk$$
$$+\cos 2\varphi\int_0^\infty(V_1{}^x-V_2{}^xk^2)\left\{-\frac{1}{r}J_1(kr)+\frac{1}{2}J_0(kr)k\right\}dk$$
$$+\cos 4\varphi\int_0^\infty V_2{}^x\left\{\left(-\frac{6}{r^2}+k^2\right)\frac{1}{r}J_1(kr)+\left(\frac{3}{r^2}-\frac{1}{8}k^2\right)J_0(kr)k\right\}dk \tag{C.1}$$

$$\frac{\Delta Y^x_{11}}{C^x_{11}}=\sin 2\varphi\int_0^\infty\left(V_1{}^x-\frac{1}{2}k^2V_2{}^x\right)\left\{-\frac{1}{r}J_1(kr)+\frac{1}{2}J_0(kr)k\right\}dk$$
$$+\sin 4\varphi\int_0^\infty V_2{}^x\left\{\left(-\frac{6}{r^2}+k^2\right)\frac{1}{r}J_1(kr)+\left(\frac{3}{r^2}-\frac{1}{8}k^2\right)J_0(kr)k\right\}dk \tag{C.2}$$

$$\frac{\Delta Z^x_{11}}{C^x_{11}}=\cos\varphi\int_0^\infty\left[\left\{V_1{}^x+\left(-\frac{2}{r^2}+\frac{1}{2}k^2\right)V_2{}^x\right\}J_1(kr)k+\frac{1}{r}V_2{}^xJ_0(kr)k^2\right]dk$$
$$+\cos\varphi\cos 2\varphi\int_0^\infty V_2{}^x\left\{\left(\frac{4}{r^2}-\frac{1}{2}k^2\right)J_1(kr)k-\frac{2}{r}J_0(kr)k^2\right\}dk \tag{C.3}$$

$$\frac{\Delta X^y_{11}}{C^y_{11}}=\sin 2\varphi\int_0^\infty\left(V_1{}^y-\frac{1}{2}k^2V_2{}^y\right)\left\{-\frac{1}{r}J_1(kr)+\frac{1}{2}J_0(kr)k\right\}dk$$
$$+\sin 4\varphi\int_0^\infty V_2{}^y\left\{\left(\frac{6}{r^3}-k^2\right)\frac{1}{r}J_1(kr)-\left(\frac{3}{r^2}-\frac{1}{8}k^2\right)J_0(kr)k\right\}dk \tag{C.4}$$

$$\frac{\Delta Y^y_{11}}{C^y_{11}}=\int_0^\infty\left(\frac{1}{2}V_1{}^y-\frac{3}{8}V_2{}^yk^2\right)J_0(kr)kdk$$
$$+\cos 2\varphi\int_0^\infty(V_1{}^y-k^2V_2{}^y)\left\{\frac{1}{r}J_1(kr)-\frac{1}{2}J_0(kr)k\right\}dk$$
$$+\cos 4\varphi\int_0^\infty V_2{}^y\left\{\left(-\frac{6}{r^2}+k^2\right)\frac{1}{r}J_1(kr)+\left(\frac{3}{r^2}-\frac{1}{8}k^2\right)J_0(kr)k\right\}dk \tag{C.5}$$

$$\frac{\Delta Z^y_{11}}{C^y_{11}}=\sin\varphi\int_0^\infty\left[\left\{V_1{}^y-\left(\frac{2}{r^2}+\frac{1}{2}k^2\right)V_2{}^y\right\}J_1(kr)k+\frac{1}{r}V_2{}^yJ_0(kr)k^2\right]dk$$
$$+\sin\varphi\cos 2\varphi\int_0^\infty V_2{}^y\left\{\left(-\frac{4}{r^2}+\frac{1}{2}k^2\right)J_1(kr)+\frac{2}{r}J_0(kr)k\right\}kdk \tag{C.6}$$

$$\frac{\Delta X^z_{11}}{C^z_{11}}=\cos\varphi\int_0^\infty\left[\left\{\left(\frac{2}{r^2}+\frac{1}{2}k^2\right)V_1{}^z+V_2{}^zk^2\right\}J_1(kr)-\frac{1}{r}V_1{}^zJ_0(kr)k\right]dk$$
$$+\cos\varphi\cos 2\varphi\int_0^\infty V_1{}^z\left\{\left(-\frac{4}{r^2}+\frac{1}{2}k^2\right)J_1(kr)+\frac{2}{r}J_0(kr)k\right\}dk \qquad \text{(C.7)}$$

$$\frac{\Delta Y^z_{11}}{C^z_{11}}=\sin\varphi\int_0^\infty\left[\left\{\left(-\frac{2}{r^2}+\frac{1}{2}k^2\right)V_1{}^z+V_2{}^zk^2\right\}J_1(kr)+\frac{1}{r}V_1{}^zJ_0(kr)k\right]dk$$
$$+\sin\varphi\cos 2\varphi\int_0^\infty V_1{}^z\left\{\left(-\frac{4}{r^2}+\frac{1}{2}k^2\right)J_1(kr)+\frac{2}{r}J_0(kr)k\right\}dk \qquad \text{(C.8)}$$

$$\frac{\Delta Z^z_{11}}{C^z_{11}}=\int_0^\infty\left(-\frac{1}{2}V_1{}^z-V_2{}^z\right)J_0(kr)k^2dk$$
$$+\cos 2\varphi\int_0^\infty V_1{}^z\left\{\frac{1}{r}J_1(kr)-\frac{1}{2}J_0(kr)k\right\}kdk \qquad \text{(C.9)}$$

With the aid of the following relations, we can dissolve apparent indefiniteness at $r=0$:

$$\lim_{r\to 0}\left\{-\frac{2}{r}J_1(kr)+J_0(kr)k\right\}=0 \qquad \text{(C.10)}$$

$$\lim_{r\to 0}\frac{1}{r^2}\left\{-\frac{2}{r}J_1(kr)+J_0(kr)k\right\}=-\frac{1}{8}k^3 \qquad \text{(C.11)}$$

We find at $r=0$:

$$\frac{\Delta X^x_{11}}{C^x_{11}}=\int_0^\infty\left\{\frac{1}{2}V_1{}^x-\frac{3}{8}V_2{}^xk^2\right\}kdk \qquad \text{(C.12)}$$

$$\frac{\Delta Y^y_{11}}{C^y_{11}}=\int_0^\infty\left(\frac{1}{2}V_1{}^y-\frac{3}{8}V_2{}^yk^2\right)kdk \qquad \text{(C.13)}$$

$$\frac{\Delta Z^z_{11}}{C^z_{11}}=\int_0^\infty\left(-\frac{1}{2}V_1{}^z-V_2{}^z\right)k^2dk \qquad \text{(C.14)}$$

$$\Delta Y^x_{11}=\Delta Z^x_{11}=\Delta X^y_{11}=\Delta Z^y_{11}=\Delta X^z_{11}=\Delta Y^z_{11}=0 \qquad \text{(C.15)}$$

References

AGGARWAL, N. P., L. P. SYKES, D. W. SIMPSON and P. G. RICHARDS, 1975, Spatial and temporal variations in ts/tp and in P wave residuals at Blue Mountain Lake, New York, *J. Geophys. Res.*, **80**, 718-732.

ANDERSON, D. L. and J. H. WHITCOMB, 1973, The dilatancy-diffusion model of earthquake prediction, in Kovach, R. L. and A. Nur (Eds.): *Proceedings of the Conference on*

Tectonic Problems of the San Andreas Fault System, Stanford Univ. Press, 417-426.

BRACE, W. F., B. W. PAULDING and C. SCHOLZ, 1966, Dilatancy in the fracture of crystalline rocks, *J. Geophys. Res.*, **71**, 3939-3956.

FISKE, R. S. and W. T. KINOSHITA, 1969, Inflation of Kilauea volcano prior to its 1967-1968 eruption, *Science*, **165**, 341-349.

GAUTSCHI, W., 1964, Error function and Fresnel integrals, in Abramowitz, M. and I. A. Stegun (Eds.): *Handbook of Mathematical Functions*, Dover Publications, New York.

GEOLOGICAL SURVEY OF JAPAN, 1979, Measurements of variations in seismic wave velocity by using explosion seismic method-preliminary report of the results in 10th (1976)-12th (1978) Oshima explosion, (*in Japanese*), *Rep. Coord. Comm. Earthquake Predict.*, **22**, 83-85.

HAGIWARA, Y., 1977a, The Mogi model as a possible cause of the crustal uplift in the eastern part of Izu Peninsula and the related gravity change, (*in Japanese with English abstract*), *Bull. Earthq. Res. Inst., Univ. Tokyo*, **52**, 301-309.

HAGIWARA, Y., 1977b, Matsushiro uplift as a multiple Mogi model, (*in Japanese with English abstract*), *J. Geod. Soc. Japan*, **23**, 25-35.

HASTINGS Jr., C., 1955, *Approximations for digital computers*, Princeton.

HILL, D. P., 1977, A model for earthquake swarms, *J. Geophys. Res.*, **82**, 1347-1352.

KISSLINGER, C., 1975, Processes during the Matsushiro, Japan, earthquake swarm as revealed by levelling, gravity, and spring-flow observations, *Geology*, **3**, 57-62.

MARTIN III, R. J., R. E. HABERMANN and M. WYSS, 1978, The effect of stress cycling and inelastic volumetric strain on remanent magnetization, *J. Geophys. Res.*, **83**, 3485-3496.

MARUYAMA, T., 1964, Statical elastic dislocations in an infinite and semi-infinite medium, *Bull. Earthq. Res. Inst., Univ. Tokyo*, **42**, 289-368.

MIZUTANI, H. and T. ISHIDO, 1976, A new interpretation of magnetic field variation associated with the Matsushiro earthquakes, *J. Geomag. Geoelectr.*, **28**, 179-188.

MJACHKIN, V. I., W. F. BRACE, G. A. SOBOLEV and J. H. DIETRICH, 1975, Two models for earthquake forerunners, *Pageoph*, **113**, 169-182.

MOGI, K., 1958, Relations between the eruptions of various volcanoes and the deformations of the ground surfaces around them, *Bull. Earthq. Res. Inst., Univ. Tokyo*, **36**, 99-134.

MOGI, K., 1985, *Earthquake Prediction*, Academic Press, 355pp.

NAGATA, T., 1970, Basic magnetic properties of rocks under mechanical stresses, *Tectonophysics*, **9**, 167-195.

NUR, A., 1972, Dilatancy, pore fluids and premonitory variations in ts/tp travel times, *Bull. Seism. Soc. Amer.*, **62**, 1217-1222.

NUR, A., 1974, Matsushiro, Japan, earthquake swarm: confirmation of the dilatancy-fluid diffusion model, *Geology*, **2**, 217-221.

NUR, A., 1975, A note on the constitutive law for dilatancy, *Pageoph.*, **113**, 197-206.

SASAI, Y., 1979, The piezomagnetic field associated with the Mogi model, *Bull. Earthq. Res. Inst., Univ. Tokyo*, **54**, 1-29.

SASAI, Y., 1980, Application of the elasticity theory of dislocations to tectonomagnetic modelling, *Bull. Earthq. Res. Inst., Univ. Tokyo*, **55**, 387-447.

SASAI, Y., 1983, A surface integral representation of the tectonomagnetic field based on the linear piezomagnetic effect, *Bull. Earthq. Res. Inst., Univ. Tokyo*, **58**, 763-785.

SASAI, Y., 1984, Magnetic change associated with a macroscopic model of crustal dilatancy—the multiple Mogi model—, (*in Japanese*), in Yukutake, T. (Ed.): *Proceedings of the 1984 Conductivity Anomaly Symposium*, 155-166.

SASAI, Y., 1985, Predominance of piezomagnetic effect in tectonomagnetic field of the Mogi model, *J. Geomag. Geoelectr.*, **37**, 159-167.

SCHOLZ, C., L. R. SYKES and Y. P. AGGARWAL, 1973, Earthquake prediction: a physical

basis, *Science*, **181**, 803-810.
SINGH, S. K., 1977, Gravitational attraction of a circular disc, *Geophysics*, **42**, 111-113.
SINGH, S. K. and F. J. SABINA, 1975, Epicentral deformation on the dilatancy-fluid diffusion model, *Bull. Seism. Soc. Amer.*, **65**, 845-854.
STACEY, F. D., 1964, The seismomagnetic effect, *Pageoph.*, **58**, 5-22.
STUART, W. D., 1974, Diffusionless dilatancy model for earthquake precursors, *Geophys. Res. Lett.*, **1**, 261-264.
TAKAHASHI, H. and M. MORI, 1974, Double exponential formulas for numerical integration, *Publ. R. I. M. S., Kyoto Univ.*, **9**, 721-741.
TAJIMA, H., 1975, Gravity change associated with earthquakes and land-deformations, (*in Japanese with English abstract*), *Bull. Earthq. Res. Inst., Univ. Tokyo*, **50**, 209-272.
VLADIMIROV, V. S., 1971, *Equations of Mathematical Physics*, (*English Translation from Russian*), Marcel Dekker.
WATANABE, H., 1984, Gradual bubble growth in dacite magma as a possible cause of the 1977-1978 long-lived activity of Usu Volcano, *J. Volcanol. Geotherm. Res.*, **20**, 133-144.
YAMAKAWA, N., 1955, On the strain produced in a semi-infinite elastic solid by an interior source of stress, (*in Japanese with English abstract*), *J. Seism. Soc. Japan* (**ii**), **8**, 84-98.
YAMAZAKI, K., 1978, Theory of crustal deformation due to dilatancy and quantitative evaluation of earthquake precursors, *Sci. Rep. Tohoku Univ., Ser. 5*, **25**, 115-167.

地殻ダイラタンシーの複合テンション・クラックモデル —その変位，重力および地磁気変化

地震研究所 笹 井 洋 一

地殻のダイラタンシー状態の巨視的モデルとして，引張り割れ目が多数，ガウス分布しているものを考えた．これは萩原 (1977b) による複合茂木モデルを拡張したものである．一個のクラックの影響は，半無限弾性体内部の適当な歪核の作用で表わされる．この影響関数にガウス分布の重みをつけて積分することによって，クラック全体の効果を表現する．更にクラックによる地表変形や密度変化によって重力が，また応力によるピエゾ磁気効果によって地磁気が，それぞれ変化する．引張り割れ目の種類として，球状のもの（いわゆる茂木モデル，T00 型），水平に置かれたクラックが上下方向に開口するもの (T33 型)，垂直なクラックが水平方向に開くもの (T11 型) を考えた．その上 T00 型モデルは，クラックがあらゆる方向に万遍無く向いているものと，力学的には等価であることが示される．求める観測量（隆起，水平変位，重力，地磁気変化）は，3 次元のたたみこみで与えられる．これをフーリエ変換を用いて変形し，ガウスの誤差関数とベッセル関数を含む，一次元積分の形に表現した．クラック分布の分散が小さい場合には，萩原の近似式が成立つ．一般の場合について，二重指数関数型積分公式を用いて，精度の良い数値積分を行なった．地表変形については，T00 型と T33 型が良く似た結果を与え，同心円状の隆起と，その数分の一の大きさの伸長を示す．一方 T11 型では，分散の値によっては二つのピークを生じ，ピークを横切る方向に隆起量より大きな水平変位を起こす．重力では T11 型で極めて大きな重力変化勾配が得られる．T11 型クラックは，もともと隆起を生ずる能力が弱い．他の二種類のクラックと同程度の隆起を生ずるのに，はるかに多くのクラック量を必要とする．T11 型の重力変化勾配が大きいのは，クラックを満たす物質の引力が大きな寄与をするためである．地磁気変化はクラックのタイプとその分布関数の違いで，かなり異なった様相を示す．T00 型では，全体として全磁力の減少が卓越する．T33 型ではほとんど地磁気変化を生じない．これは T33 型クラックの作るピエゾ磁気が，クラックの位置より浅い部分と深い部分とで，互いに打消し合うように生ずるからである．T11 型で東西走向のクラックの場合には，全磁力の増加域も現われる．クラック分布の水平方向の分散が大きくなると，地磁気変化は急速に小さくなる．またクラック分布の中心が深くなっても，同様な影響がある．結局，活断層近傍の応力集中によって，局所的かつ浅い部分に，T00 型又は T11 型のクラックを生じた場合にだけ，顕著な地磁気変化が期待できることになる．ここで考えたモデルは，空隙を満たした物質が，クラックを押し拡げる場合に，最も良くあてはまる．ダイラタンシー＝水拡散説における水の代りに，マグマや火山ガスが間隙物質になる火山現象には，このモデルで近似できるものが多い．火山性群発地震の発生機構として提案された Hill (1977) のモデルは，卓越走向を持つダイクから成り，T11 型で記述できる．またシルやダイクの集合から成るマグマ溜りや，火山性地殻変動の力源モデルにも適用可能である．